
μ CRASP: Multimodal Chain-of-thought Reasoning aware Structured Pruning

Aritra Dutta

Somak Aditya

Indian Institute of Technology (IIT), Kharagpur

Abstract

Vision-language models (VLMs) increasingly rely on chain-of-thought (CoT) reasoning to solve complex multimodal tasks, but their large parameter sizes make deployment comparably expensive. Structured model pruning methods offer a natural solution. However, existing methods fail to preserve CoT reasoning accuracy when applied to VLMs. We identify two reasons: i) CoT reasoning consistency is governed by sparse transition points (pivot tokens) in the generation trajectory, and conventional pruning methods are CoT-agnostic; and ii) traditional pruning designed for unimodal LLM’s does not account for the activation distribution difference across the visual and textual modalities, making pruning significantly more challenging than in purely textual unimodal models. Based on this insight, we propose μ CRASP, a structured pruning framework that explicitly targets reasoning-critical components while preserving cross-modal alignment and accounting for layer-wise sensitivity under a global parameter budget. Our approach enables effective compression while maintaining both reasoning coherence and multimodal grounding. Experiments on four VLMs across three reasoning benchmarks show that μ CRASP consistently preserves reasoning quality under increasing compression. At 30% pruning on Qwen2.5-VL-7B, CoT generated under μ CRASP retains a high consistency with original (dense) finetuned model compared to best pruning baselines - with LLM-Judge score of 8.87 vs 7.32 on physical reasoning on a scale of 0 – 10. It further sustains high reasoning consistency (LLM-J > 7.0) up to 50% pruning, a 20 – 25 percentage-point improvement over existing methods. Notably, existing pruning methods suffer from abrupt performance collapse beyond 25 – 30% pruning, whereas our method maintains high logical validity under LLM-as-judge evaluation and stable semantic similarity even up to 50% pruning levels, while exhibiting comparably lower degradation in perplexity.

1 Introduction

In recent years, we have witnessed massive advances in multimodal reasoning through efficient vision and language modeling with systems such as, Qwen2.5-VL [34], Gemma-3 [7], and LLaVA-OneVision [23]; which integrate heavily pretrained vision encoders with powerful (large) language decoders. Augmented by techniques like Chain-of-Thought prompting [43, 19], these models now exhibit strong performance across demanding applications; including medical visual question answering, autonomous driving, and scientific diagram reasoning, where structured, step-by-step inference is essential. A critical enabler of this performance is chain-of-thought (CoT) prompting [43, 19], which elicits explicit intermediate reasoning steps before a final answer. Following the success in text-based reasoning Wei et al. [43], various works adapted CoT to the multimodal context using text-only CoT [49, 45] and CoT with visual context (bounding boxes [36] or visual tokens [5]). However, since large(r) models benefit from CoT more [43], this comes with a substantial computational burden, posing significant challenges for real-world deployment. Although model

pruning offers a promising route toward efficiency, existing methods largely overlook the inherently structured, multi-step nature of chain-of-thought reasoning in multimodal contexts, leading to brittle performance under compression.

Therefore, our central objective in this work is to preserve multimodal CoT reasoning abilities of VLMs under extreme compression. We specifically adopt the text-only variant as *multimodal chain-of-thought (CoT) reasoning*, representing the process of answering questions about an image through a sequence of intermediate *text-based* reasoning steps grounded in both visual and textual inputs. To investigate *reasoning* skills, we particularly focus on visual reasoning (or question-answering) benchmarks which require such multi-step reasoning to solve. For example, questions such as “*If the glass near the table edge is bumped, will water spill onto the laptop below?*” require identifying spatial relationships, applying physical reasoning, and chaining these observations into a causal conclusion.

This problem is challenging and under-explored for two key reasons. *First*, current pruning methods do not explicitly cater to preserving *reasoning coherence* in CoT. Existing methods such as Wanda [38], SparseGPT [6], and LLM-Pruner [26] estimate importance via aggregate loss, treating all tokens equally. In long CoT responses, only a small subset of tokens correspond to reasoning transitions, and their contribution is diluted under such aggregation, leading to a signal-to-noise imbalance. *Second*, VLMs introduce additional complexity beyond LLMs due to cross-modal entanglement, architectural heterogeneity, and large disparities in unit granularity across components. As a result, pruning decisions must account not only for reasoning structure but also for preserving vision-language alignment. Motivated by these challenges, we investigate three questions: **(RQ1)** Can structural pruning preserve the logical coherence of multi-step CoT reasoning in VLMs? **(RQ2)** Why do existing pruning methods fail to preserve reasoning when applied to VLMs? **(RQ3)** How should pruning be redesigned to preserve reasoning trajectories under strict parameter budgets?

Overall, we make the following contributions:

1. **Failure of traditional pruning methods in VLMs.** We show that structured pruning methods (e.g., FLAP, LLM-Pruner, Attribution Pruning [2, 26, 44]) fail to preserve chain-of-thought (CoT) reasoning in VLMs despite sometimes maintaining acceptable perplexity. These methods treat all CoT tokens uniformly and ignore cross-modal interactions, causing reasoning chains to collapse under moderate compression.
2. **A reasoning-aware, training-free pruning method for VLMs.** We introduce μ CRASP—a multimodal CoT reasoning aware (training-free) pruning method, that is targeted to preserve chain-of-thought reasoning quality in VLMs under high structural compression. μ CRASP integrates reasoning-aware attribution to capture transition-critical (*anchor*) tokens in CoT, cross-modal dependency modeling to retain vision–language alignment, and layer-wise sensitivity to guide structured pruning under a global parameter budget.
3. **Extensive benchmarking and analysis for the preservation of reasoning quality.** At different levels of pruning, we benchmark the performance of our method against four pruning baselines on four VLMs across three datasets. We estimate *logical validity* of chain-of-thought (CoT) using an LLM-as-a-judge metric [51, 4], and report other final answer-level metrics. Furthermore, our extensive analysis involving MLP zero-out, *anchor* token ablation, and distributional differences between next token prediction abilities before and after pruning pinpoints how each component of our method supports CoT quality preservation during high pruning levels.

2 Related Work

Structured vs. Unstructured pruning. Neural network pruning research has a long history, spanning early approaches such as optimal brain damage [21], optimal brain surgeon [12] to modern large-scale methods. Among these, unstructured methods operate by zeroing individual weights. SparseGPT [6] solves layer-wise sparse regression to achieve 60% sparsity on 175B models with negligible accuracy loss; Wanda [38] uses the product of weight and activation magnitude for efficient one-shot pruning. However, this may result in irregular sparsity patterns, which require specialized hardware for inference speedup. In contrast, structured methods remove entire units (neurons, heads, layers), producing dense sub-networks with direct hardware acceleration. LLM-Pruner [26] uses Taylor-based dependency graphs; SliceGPT [3] projects weight matrices to lower dimensions; and FLAP [2] measures activation fluctuation.

Layer-wise vs. Global pruning. Layer-wise methods, including SparseGPT and Wanda, determine per-layer masks by minimizing local reconstruction error independently. This is computationally convenient, but locally optimal decisions need not compose globally. Global methods [31, 32] rank all units across the network by a single importance score. ECoFLaP [39] bridges the two via zeroth-order global importance for per-layer sparsity ratios. OWL [47] uses outlier distributions for non-uniform sparsity. We adopt global pruning because VLM structural unit costs span orders of magnitude ($\sim 5.2\text{M}$ per GQA group vs. $\sim 21\text{K}$ per MLP neuron), and a global knapsack formulation [29] naturally handles this heterogeneity.

VLM Compression. Previous work on VLM pruning is somewhat limited and focuses mainly on token-level pruning of visual inputs (e.g., ATP-LLaVA [46], IVTP [15]) or intrinsic dimension-based methods [42]. These methods operate at the input or activation level without structurally pruning parameters. Among parameter-level approaches, ECoFLaP [39] handles BLIP-style architectures for captioning and simple VQA. TAMP [18] introduces token-adaptive layer-wise sparsity. To the best of our knowledge, no prior work studies structured pruning of VLMs with the explicit objective of preserving chain-of-thought reasoning.

Chain-of-Thought (CoT) reasoning. The simple technique of CoT prompting [43, 19] has shown drastic improvements in the reasoning ability of LLMs. Following the success, researchers adopted CoT in multimodal setting [50], where the CoT grounds rationales in visual evidence [24]. To improve latency and token efficiency, researchers have worked on reducing redundancy [25], preference-based CoT optimization [48], and attention-head specialization [41, 30]. Knowledge distillation approaches for compressing reasoning capabilities [13, 14] are complementary to our pruning framework and can serve as a post-pruning recovery stage. However, no prior work explicitly studies how pruning affects the structural integrity of generated reasoning chains.

3 Problem Setup: Structured Pruning for Multimodal CoT Reasoning

We consider the CoT reasoning task in Vision-Language Model (VLM), where a VLM is explicitly prompted to answer a question about an image in a step-by-step fashion. Specifically, given an image and a question as input, we use a CoT prompt [43] to instruct the VLM ($M = (\mathcal{E}_v, \mathcal{D}_\ell)$) to generate a chain of intermediate reasoning steps before producing a final answer. Intermediate steps, as well as the final answer are sequentially sampled from the model conditioned on previous steps and the input.

Structured Pruning of VLMs. For pruning, we assume the VLM $M = (\mathcal{E}_v, \mathcal{D}_\ell)$ consists of a vision encoder \mathcal{E}_v with l_v transformer blocks and a language decoder \mathcal{D}_ℓ with l_ℓ transformer layers. Each module contains *structural units* (\mathcal{U}_ℓ): individual neurons for SwiGLU MLPs (a gated MLP variant used in modern transformers) [37], attention heads for vision blocks, and GQA groups [1] for language attention (for more details, refer Appendix).

We further assume that the importance of the task-based individual network parameter is calculated using the standard First-order Taylor expansion [31, 32]. Here, for a structural unit u with weight vector \mathbf{w}_u , importance of the unit is approximated as the change in loss upon removal of the unit, given by: $\Delta\mathcal{L} \approx \mathbf{w}_u^\top \nabla_{\mathbf{w}_u} \mathcal{L}$. We take absolute values to ensure non-negative importance, and aggregate over a calibration dataset \mathcal{D} to yield a global importance score. This forms the backbone of structured pruning methods for traditional neural networks and LLMs [26], as well as our approach.

4 Our Method: μ CRASP

Given a VLM M and a target pruning ratio S , our goal is to identify and remove structural units, that contribute least to chain-of-thought reasoning quality, while respecting a global parameter budget. Our algorithm operationalizes two hypotheses: 1) we *posit* that there are a few important transition regions (marked by *anchor* tokens) in CoT which are crucial for governing reasoning coherence, and 2) a VLM-aware pruning method must take the activation distribution difference between vision and language components.

Algorithm. We define our method μ CRASP as a sequence of four principal steps (Fig 1).

First, for each structural unit, we compute a standard global attribution score I_{global} via first-order Taylor expansion over all token positions (AppendixB.1).

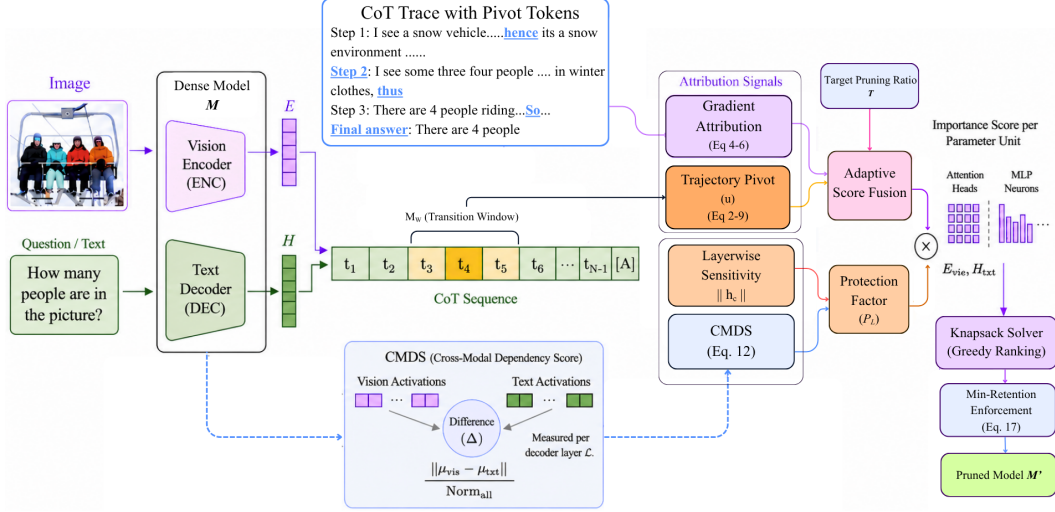


Figure 1: **Overview of μ CRASP.** Gradient attribution and trajectory-pivot attribution provide complementary pruning signals, which are fused using a pruning-ratio-dependent coefficient γ_{dyn} . Per-layer cross-modal dependency (CMDS) and output sensitivity define a protection factor p_f that preserves vision-language integration layers under aggressive pruning. The resulting importance scores are used by a greedy knapsack solver to allocate the global pruning budget across attention heads and MLP neurons while enforcing minimum retention constraints.

Second, we compute trajectory pivot attribution score A_{pivot} by restricting attribution to local windows around detected transition regions (AppendixB.2). These transition regions are, in turn detected by identifying a few *pivot* (or reasoning transition) *tokens*, which occur near boundaries between successive reasoning steps. These tokens correspond to points where the model consolidates the conclusion of one intermediate step and initiates the next. For example, in a multi-step visual reasoning task, a transition may occur when the model shifts from describing observed entities (e.g., identifying objects or spatial relations) to making an inference or causal conclusion. Empirically, such transitions are sparse ($\approx 5\%$ of tokens) yet disproportionately important, as perturbing them disrupts logical continuity. To approximate these transition points, we apply a lightweight detection strategy that identifies two classes of surface markers: *structural delimiters*, such as numbered step prefixes (“Step 1:”, “2.”) and terminal markers (“Final Answer:”, “Conclusion:”,); and *logical connectives*, such as causal or conclusory conjunctions (“Therefore”, “Thus”, “So”, “Hence”, “This means”, “and” etc). When neither classes of markers is present, we resort to considering tokens at sentential boundaries. Despite the heuristic, our overall method is resistant to variations in choice of structural patterns, as i) we depend on conventional linguistic and structural cues, ii) we define a window of W tokens around the markers, and iii) the rest of our method ensures a dependency on the transition *region(s)* than specific tokens (later validated by experiments in Appendix A.1).

Third, we quantify cross-modal affinity of each decoder layer using a *Cross-Modal Dependency Score* (CMDS) –a measure inspired by Maximum Mean Discrepancy (MMD) [10]. MMD is a kernel-based statistical distance between probability distributions; motivated by this formulation, we formulate it to quantify the discrepancy between activation distributions induced by visual and textual tokens within a layer. This allows CMDS to capture the extent to which a layer contributes to cross-modal interaction, rather than merely measuring distributional differences in a generic sense (AppendixB.3). We additionally measure structural load via output activation magnitude (AppendixB.4).

Fourth, we fuse I_{global} and A_{pivot} with a compression-conditioned mixing coefficient γ_{dyn} that progressively decreases the reasoning-specific signal as the parameter budget tightens. Here, we additionally factor in individual layer-wise activation distribution (aka *sensitivity*) as well as CMDS scores. Therefore, we scale the resulting importance by layer-level protection factors derived from CMDS and *sensitivity* (AppendixB.5).

Objective. Lastly, we solve a global knapsack problem over all structural units, ranking them by value-to-cost efficiency and selecting units greedily until the parameter budget is met, with minimum-retention constraints to prevent layer collapse. This formulation is necessary due to the extreme heterogeneity of structural units in VLMs: for example, a single GQA group in Qwen2.5-VL-7B contains $\sim 5.2\text{M}$ parameters, whereas an MLP neuron contains only $\sim 21\text{K}$. Uniform layer-wise pruning leads to disproportionate removal of low-cost units while retaining expensive ones. By contrast, global allocation optimizes the trade-off between importance and parameter cost across all units. Given the target pruning ratio $S \in (0, 1)$, we retain a subset of structural units (a keep-set $\mathcal{K} \subseteq \bigcup_{\ell} \mathcal{U}_{\ell}$), which maximizes reasoning-preserving importance by satisfying:

$$\max_{\mathcal{K} \subseteq \bigcup_{\ell} \mathcal{U}_{\ell}} \sum_{u \in \mathcal{K}} I(u) \quad \text{subject to} \quad \sum_{u \in \mathcal{K}} c(u) \leq (1 - S) \sum_{u \in \bigcup_{\ell} \mathcal{U}_{\ell}} c(u), \quad (1)$$

where $I(u)$ denotes the (reasoning-aware) importance of unit u , $c(u)$ is the parameter count of unit u . We provide more details of the four components: global attribution in AppendixB.1, trajectory pivot attribution in AppendixB.2), layer-level profiling via CMDS and sensitivity in AppendixB.3 & B.4), and dynamic fusion with global knapsack allocation in AppendixB.5). Fig 1 provides an overview and Algorithm 1 gives the complete procedure.

5 Experimental Setup

We design experiments to address three questions: *Can* structural pruning preserve CoT reasoning in VLMs (RQ1)? *Why* do existing pruning methods fail at this task (RQ2)? And *how* does reasoning-aware pruning overcome these failures (RQ3)? Each design decision-choice of metrics, benchmarks, architectures, and baselines-targets one or more of these questions.

Architectures: spanning model families and scales. We evaluate four VLMs that span three architectural families and a large parameter range: *LLama 3.2-11B* [8] (10.1B, 40 layers), *Qwen2.5-VL-7B* [34] (7.9B, 28 layers), *Gemma-3-4B* [7] (4.3B, 34 layers), *Qwen2.5-VL-3B* (3.8B, 36 layers), and *Qwen2-VL-2B* [33] (2.2B, 28 layers). The Qwen family uses a ViT-based encoder with patch merging, while Gemma uses SigLIP with pooling-based projection, spanning various VL fusion architectures. All models employ grouped-query attention (GQA) (Appendix Table J).

Datasets: testing visual grounding and reasoning across domains. We select three datasets, each concentrating on a different facet of visually grounded multi-step reasoning and ensuring that our evaluation is not dominated by a single reasoning type: (1) *TDIUC-Physical* [16] requires reasoning about spatial layout, colour, shape, and material properties - tasks where the model must ground each reasoning step in specific visual features. (2) *TDIUC-Quantitative* [16] requires counting, numerical comparison, and arithmetic inference, testing whether pruning disrupts the precise token-level operations needed for numerical answers. (3) *A-OKVQA* [35] requires commonsense reasoning grounded in visual scenes (25K questions over COCO), testing whether pruning destroys the broadly distributed world knowledge that supports commonsense inference. For each dataset, we generate CoT traces using GPT-4o, validate using manual evaluation and consider it as ground-truth trace. We use the held-out test sets for evaluation. For further details, see Appendix D & F.

Metrics: evaluating reasoning, not just token accuracy. Prior pruning work evaluates compressed models almost exclusively via perplexity, BLEU, F1, or direct-answer accuracy [26, 2, 6]. These metrics capture surface-level fluency and lexical overlap, but do not quantify logical validity of reasoning steps after pruning. To address this gap, we introduce **LLM-as-Judge (LLM-J)** as one of our key metric. Here, we use GPT-3.5-TURBO to evaluate the logical validity of each generated CoT trace against the ground-truth chain and assigns a score on a 0-10 scale¹(AppendixG.4).

We complement LLM-J with six additional metrics that capture distinct failure modes. **Perplexity (PPL)** measures token-level prediction confidence. **Exact Match (EM_a)** and **Semantic similarity (SEM_{c+a})** test of the CoT + final answer precision respectively. **Formatting Score** verifies structural integrity of the CoT trace; and **BLEU** and **F1** provide standard surface-level baselines. These metrics help us disentangle reasoning collapse from answer-extraction failure.

¹In Appendix G.4, we justify the choice of the scale with a comparative analysis.

Pruning Baselines & Calibration Protocol. We construct a calibration set by randomly sampling 128 image, question pairs from the training split and pairing them with synthetic CoT traces generated by GPT-4o (Appendix F). We use the same calibration set for all the baselines and our method.

We compare against five structured pruning methods, all using our calibration set: (1) **Magnitude**: removes units with smallest aggregate ℓ_1 weight norm [52]. (2) **Attribution Pruning**: task-specific gradient-based saliency [44], providing a stronger task-aware baseline. (3) **LLM-Pruner**: dependency-graph-based group pruning with first and second-order Taylor importance [26]. (4) **Wanda-SP**: the structured variant of Wanda [38] as implemented by [2], using the product of weight magnitude and input activation norm. (5) **FLAP**: fluctuation-based adaptive structured pruning [2]. We provide further details of the baselines in Appendix E.

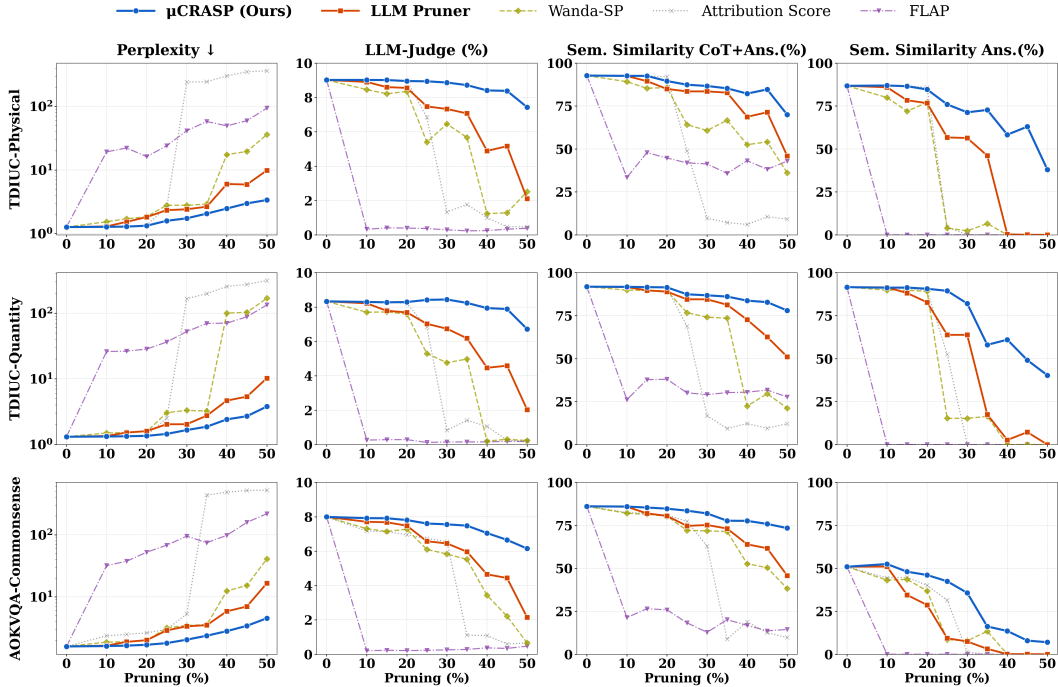


Figure 2: Performance across pruning methods under increasing pruning level on Qwen2.5-VL-7B across three reasoning domains. Each row corresponds to a domain; columns report Perplexity, LLM-Judge, Semantic Similarity (cosine) of CoT + final answer, and Semantic similarity (semantic) of final answer. We report Magnitude Pruning [22] results in Appendix C, due its low performance.

6 Experimental Results: Compression vs. Performance

We report the compression vs./ performance curves for Qwen2.5-VL-7B in Fig.2 and cross-model results at 30% pruning across all four VLMs in Table 1. Full compression–performance curves for all four VLMs with additional token level metrics are provided in Appendix L.

We organize the findings around three themes that hold *in all models*.

μ CRASP preserves reasoning coherence while exact-match accuracy degrades first.

We observe that across all four VLMs, LLM-J and EM_a follow *visibly* different degradation trajectories under μ CRASP. LLM-J degrades minimally even at high pruning ratio, while EM_a collapses much earlier and more steeply. In Qwen2.5-VL-7B (Physical), the unpruned model receives an

¹In Table 1 EM_a is computed using strict token-level string matching between the predicted and ground-truth final answer. As a result, semantically correct but syntactically verbose responses receive zero score despite conveying the correct answer. we therefore additionally report Semantic Similarity (SEM_{c+a}) in table and other token level metrics in the model compression-performance curves in Appendix L.

Table 1: μ CRASP versus baselines at 30% **pruning ratio** across four VLMs and three reasoning domains. We report LLM-Judge (J), String match of final Answer (EM_a), Semantic Similarity (cosine) of CoT + final Answer (SEM_{c+a}), Perplexity (PPL) and the unpruned model performance *Dense M*. We have put *INF* where the PPL value is more than 1K.

#	Method	Physical				Quantitative				Commonsense			
		J	EM_a	SEM_{c+a}	PPL	J	EM_a	SEM_{c+a}	PPL	J	EM_a	SEM_{c+a}	PPL
Llama 11B	Dense M.	8.85	85.8	91.82	1.44	7.91	89.3	90.88	1.44	7.8	51.7	85.6	1.72
	μ CRASP	8.55	80.7	89.72	1.80	7.29	79.8	87.01	1.88	6.66	34.9	80.41	2.39
	LLM-Pruner	4.69	0.0	65.62	3.57	2.44	0.0	54.46	3.89	2.77	0.0	55.41	4.96
	Wanda-SP	5.0	0.0	60.45	3.21	3.02	0.0	57.46	3.60	4.43	0.0	57.95	4.63
	Attribution P.	8.07	0.0	85.61	2.41	5.78	9.46	76.77	2.49	6.95	23.93	79.99	2.81
	FLAP	2.79	0.0	56.33	5.98	3.41	0.0	47.66	7.18	2.02	0.0	44.90	12.2
Qwen 7B	Dense M.	9.01	86.73	92.69	1.26	8.33	91.6	91.85	1.31	8.0	50.9	86.07	1.58
	μ CRASP	8.87	71.3	86.64	1.74	8.44	82.1	86.84	1.66	7.56	35.72	81.93	2.0
	LLM-Pruner	7.32	56.4	83.48	2.41	6.74	63.8	84.51	2.03	6.45	7.4	75.19	3.4
	Wanda-SP	6.45	2.4	60.74	2.79	4.76	15.2	74.15	3.31	5.83	7.9	71.78	3.5
	Attribution P.	1.33	0.0	9.72	241	0.08	0.0	16.78	166.6	6.56	1.31	62.91	5.3
	FLAP	0.3	0.0	41.28	41.47	0.02	0.0	29.07	52.49	0.2	0.0	12.78	95.1
Gemma 4B	Dense M.	8.65	83.53	92.06	1.28	7.85	90.23	91.08	1.38	7.02	46.55	84.31	1.71
	μ CRASP	8.02	77.3	88.71	1.9	6.95	87.4	87.89	2.1	6.26	31.7	80.03	2.4
	LLM-Pruner	0.78	0.1	40.37	11.9	0.45	0.0	42.74	10.5	0.67	0.0	38.67	10.4
	Wanda-SP	1.92	0.1	52.85	3.5	1.61	1.3	62.56	3.51	1.29	0.7	54.83	4.9
	Attribution P.	7.72	73.4	86.18	2.12	6.94	83.8	85.55	2.3	6.19	28.4	78.57	2.4
	FLAP	0.3	0.0	35.06	17.7	0.04	0.0	25.76	49.87	0.09	0.0	8.89	44.2
Qwen 3B	Dense M.	8.86	85.97	92.08	1.36	8.33	91.6	91.85	1.31	7.50	49.08	84.95	1.74
	μ CRASP	8.07	24.8	80.64	2.57	7.51	41.0	83.79	2.35	6.70	23.1	77.54	3.4
	LLM-Pruner	6.73	0.1	64.61	3.49	5.64	0.0	60.35	3.12	5.11	0.0	62.78	3.5
	Wanda-SP	5.34	0.0	59.96	7.47	0.5	0.0	53.77	21.27	3.63	0.2	50.36	18.9
	Attribution P.	0.01	0.0	3.77	<i>INF</i>	0.01	0.0	5.05	<i>INF</i>	0.02	0.0	8.80	<i>INF</i>
	FLAP	0.03	0.0	32.49	66.9	0.06	0.0	38.09	40.43	0.05	0.0	27.76	99.2
Qwen 2B	Dense M.	8.39	78.37	90.04	1.76	7.55	87.45	89.35	1.8	6.97	39.65	81.98	2.21
	μ CRASP	7.65	63.4	86.98	2.4	6.65	52.0	83.55	2.37	5.3	13.9	76.02	3.8
	LLM-Pruner	5.35	0.0	72.57	4.6	4.39	0.6	68.76	3.84	4.91	0.4	69.10	4.2
	Wanda-SP	0.29	0.0	25.60	15.6	0.9	0.0	18.90	12.92	0.6	0.0	10.36	17.4
	Attribution P.	7.17	17.2	81.17	2.7	6.26	13	74.84	2.71	5.21	5.9	72.57	3.5
	FLAP	0.9	0.0	39.76	15.5	0.7	0.0	35.08	17.7	1.13	0.0	34.80	20.7

LLM-J score of 9.02 and EM_a of 86.7. At 30% pruning, LLM-J drops by only 0.15 points to 8.87, while EM_a drops by 15.4 points to 71.3. The asymmetry is more stark on smaller models: Qwen2.5-VL-3B at 30% retains LLM-J 8.07 (−9% from dense 8.86), but EM_a collapses from 86.0 to 24.8 (−71%); similarly, Qwen2-VL-2B at 40% pruning holds LLM-J at 6.93 while EM_a falls to 14.0. Interestingly, we observe this behavior distinctively for μ CRASP, and not other pruning methods. For example, when Gemma-3-4B’s reasoning collapses under LLM-Pruner beyond 20% pruning ratio (LLM-J: 6.77 \rightarrow 0.54 at 25%), EM_a drops simultaneously from 50.8 to 0.03. Likewise, Qwen2.5-VL-3B under FLAP collapses at just 10% pruning ratio (LLM-J 0.37, EM_a 0.03), with no separation between the two metrics. This indicates that, μ CRASP treats reasoning coherence as a *separable* capability, preserving logical chain structure even as the verbatim precision of the final answer degrades.

Scaling behaviour across model sizes. We compare μ CRASP against the best available baseline on the largest and smallest models at 30% pruning in Table 1. On Qwen2.5-VL-7B, μ CRASP improves LLM-J by +1.54, +1.70, and +1.0 points on Physical, Quantitative, and Commonsense respectively, while simultaneously recovering +14.9, +18.2, and +34.4 points of exact-match accuracy (EM_a). On the 2B model, LLM-J gains are more modest (+0.48, +0.39 points on Physical and Quantitative), but the EM_a improvements are +46.2 and +39.0 points, indicating that μ CRASP preserves answer-extraction capability even when reasoning coherence is partially degraded by compression. These

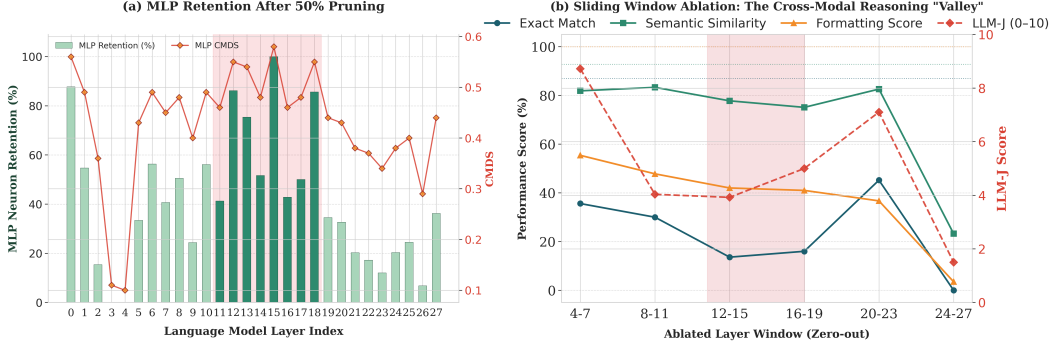


Figure 3: (a) MLP neuron retention after 40% pruning (bars) overlaid with per-layer MLP CMDS (red line). Layers in the peak CMDS region (11 – 18) retain substantially more neurons. (b) Sliding window ablation on Qwen2.5-VL-7B Physical: zeroing out four contiguous layers at each position. Ablating low-CMDS layers (4-7) causes only moderate degradation, whereas ablating high-CMDS layers (12-15, 16-19) triggers catastrophic structural collapse across all metrics, confirming that CMDS correctly identifies the cross-modal bottleneck.

results confirm that μ CRASP’s gains are robust across model scales. For smaller models, μ CRASP achieves consistently large EM_a gains with moderate LLM-J improvements. Qualitative example of generated reasoning traces for our method and baselines at 50% pruning are shown in Appendix M.

Domain-specific degradation patterns are consistent across model scales. We observe that Physical reasoning degrades the slowest. Here, all four models retain LLM-J within 10% of their dense baseline at 30% pruning (Qwen2.5-VL-7B: 8.87 vs dense 9.02; Gemma-3-4B: 8.02 vs./ 8.65; Qwen2-VL-2B: 7.65 vs./ 8.39). For quantitative reasoning, μ CRASP preserves reasoning coherence to a large extent while losing numerical precision: LLM-J remains high at 30% (Qwen2.5-VL-7B: 8.44; Gemma-3-4B: 6.95) while EM_a drops sharply beyond this point (Qwen2.5-VL-7B: 82.1 \rightarrow 61.0 at 40%; Qwen2-VL-2B: 52.0 \rightarrow 2.1 at 40%). Commonsense reasoning declines most uniformly, with LLM-J decreasing at a near-constant rate through 40% pruning on both larger models Qwen2.5-VL-7B: 7.56 \rightarrow 7.05; Gemma-3-4B: 6.26 \rightarrow 5.65 and without the steep declines seen in baselines. Collectively, these experiments show that μ CRASP’s compression behavior is governed by the structural demands of each reasoning type, not by model or domain-specific factors.

7 Analysis

a) CMDS identifies and shields the cross-modal bottleneck. In Fig 3(a), we present the CMDS scores across all 28 decoder layers of Qwen. For MLPs, CMDS remains low in the early layers (0.09–0.36 for layers 3–7), rises sharply in the middle layers 11–18 (reaching 0.61 at layer 15 and 0.60 at layer 18), and declines again toward the final layers. This pattern reflects a progression from modality-agnostic token processing in early layers, to vision-language fusion (*grounding*) in the middle, and finally to prediction-focused computation (*reasoning*) in the later stages. μ CRASP leverages this signal to allocate its retention budget. Beyond 40% pruning, it preserves 60–100% of MLP neurons in the peak-CMDS region, while retaining only 5–15% in low-CMDS layers (1–7) (Fig 3(a)). In contrast, SOTA pruning baselines ignore this pattern. For instance, Wanda-SP and Attribution Pruning prune the middle layers indiscriminately, disrupting vision-language coupling. On Qwen2.5-VL-7B, Attribution Pruning induces a sharp perplexity increase from 2.57 to 241 between 25% and 30% pruning ratio, indicating catastrophic failure due to removing units critical for cross-modal integration. Moreover, our ablations in Appendix A.1 show that removing CMDS causes sharp performance degradation in our framework.

But, does CMDS identify the true bottleneck? To verify that CMDS correctly identifies cross-modal bottlenecks, we conduct a layer-wise ablation experiment. Using 500 random samples from the Physical domain, we zero out the MLP weights of four contiguous layers at five sliding-window

positions across the decoder (Figure 3(b))². Here, initial layers (4 – 7) with low CMDS scores cause graceful degradation: Semantic Similarity (SEM_{c+a}) remains high ($\sim 83\%$), Formatting Score stays near 57%, and LLM-J holds at ~ 8.8 – the model still reasons coherently but over corrupted early-stage features. When we zero out layers with high CMDS scores (12–15 or 16–19), this triggers a qualitatively different failure: the formatting score collapses, semantic similarity crashes, and LLM-J drops sharply. These failure modes confirm that layers 11–18 serve specifically as the structural bottleneck for multimodal reasoning, and pruning them severs the network’s ability to integrate visual context into the linguistic reasoning trajectory. μ CRASP’s CMDS-based protection dynamically shields precisely this region, which explains why it sustains reasoning quality where baselines that distribute pruning uniformly across layers cannot.

b) Pivot attribution protects reasoning-transition tokens. At 30% pruning on Qwen2.5-VL-7B Physical, μ CRASP achieves an LLM-J score of 8.9 while the strongest remaining baseline, LLM-Pruner, reaches only 7.3, and Attribution Pruning collapses to 1.3. The gap between μ CRASP and LLM-Pruner is not explained by overall token-prediction quality. Both methods operate under the same parameter budget and report similar perplexity what differs is which tokens drive their respective importance scores. Methods that aggregate attribution uniformly across all positions preserve units responsible for fluent next-token prediction while discarding those that maintain logical structure across reasoning steps, because reasoning-transition tokens constitute only $\sim 5\%$ of the sequence and their signal is diluted under uniform aggregation. Trajectory pivot attribution corrects this by concentrating importance on tokens at step boundaries and reasoning transitions ensuring the keep-set retains units critical for inter-step coherence rather than only for surface-level fluency.

c) μ CRASP preserves the dense model’s output distribution. We further verify that μ CRASP preserves the dense model’s token-level predictive distribution by measuring per-token KL divergence $D_{KL}(p_{\text{dense}} || p_{\text{pruned}})$ over the full vocabulary on 512 calibration samples at 30% pruning (Fig. 4). μ CRASP achieves the lowest mean KL divergence (0.92 nats/token), outperforming the next-best baseline, LLM-Pruner (1.53), by $1.7\times$ and Attribution Pruning (10.51) by $11.4\times$. Its KL density remains sharply concentrated near zero across all domains, indicating near-identical logit distributions between dense and pruned models. In contrast, Wanda-SP and FLAP exhibit substantially broader divergence profiles, while Attribution Pruning shows severe bimodal drift, consistent with its catastrophic perplexity at 30% pruning ratio. These trends closely mirror the LLM-J results in Section 6, suggesting that μ CRASP preserves the underlying logit geometry rather than merely surface-level textual similarity. Full distributional analysis with the plot is in Appendix A.5.

d) Why does μ CRASP generalize across reasoning domains? μ CRASP delivers consistent LLM-Judge improvements over the strongest baseline (LLM-Pruner) across all three reasoning domains at 30% pruning, with mean gains of +3.1 on Physical, +3.1 on Quantitative, and +2.2 on Commonsense (all on a 0–10 scale), averaged across all four VLMs. The improvement is not concentrated in a single reasoning type or model scale: gains are positive in every one of the twelve model–domain pairs, with the smallest observed delta being +0.35 (Qwen2-VL-2B, Commonsense) and the largest +7.2 (Gemma-3-4B, Physical, where all baselines collapse). Across all model–domain pairs at 30% pruning, μ CRASP achieves an overall mean LLM-J of 7.3 versus 4.6 for LLM-Pruner, a +2.8 point improvement. The key takeaway is that CMDS-aware pruning and pivot attribution jointly provide a *domain-agnostic* benefit: by protecting the architectural structures responsible for cross-modal integration and reasoning transitions, μ CRASP preserves CoT quality regardless of which reasoning capability the benchmark exercises.

8 Conclusion

We introduced μ CRASP, a structured pruning framework for VLMs that preserves chain-of-thought reasoning under high compression. The core insight is that CoT coherence is governed by sparse pivot tokens at reasoning-step boundaries whose importance is diluted under the token-uniform aggregation used by prior methods [26, 2, 38, 6]. μ CRASP corrects this by combining pivot-restricted Taylor attribution with a Cross-Modal Dependency Score [10] that shields vision–language integration layers from aggressive pruning, two protections absent from prior VLM compression work [39, 18, 42]. At 50% pruning the gap widens further: μ CRASP retains a mean LLM-J of 3.90 while LLM-Pruner falls to 1.56, demonstrating that μ CRASP degrades where baselines collapse. Our

²Performing MLP zero out ablation per layer, does not show the degradations properly. Therefore, we group consecutive layers for this experiment.

analysis additionally reveals that reasoning coherence and answer-extraction accuracy degrade along fundamentally different trajectories under μ CRASP, logical chain structure is preserved long after verbatim answer precision begins to deteriorate; a decoupling that never occurs in any baseline and that motivates richer evaluation protocols for compressed generative models [20]. μ CRASP performs no fine-tuning. And, we leave post-pruning recovery methods such as knowledge distillation [13] or parameter-efficient adaptation to future work.

References

- [1] Joshua Ainslie, James Lee-Thorp, Michiel de Jong, Yinfei Yang, Siddhartha Jayanti, and Santiago Ontañón. GQA: Training generalized multi-query transformer models from multi-head checkpoints. In *EMNLP*, 2023.
- [2] Yongqi An, Xu Zhao, Tao Yu, Ming Tang, and Jinqiao Wang. Fluctuation-based adaptive structured pruning for large language models. In *AAAI*, 2024.
- [3] Saleh Ashkboos, Maximilian L. Croci, Marcelo Gennari do Nascimento, Torsten Hoeffler, and James Hensman. SliceGPT: Compress large language models by deleting rows and columns. In *ICLR*, 2024.
- [4] Guiming Hardy Chen, Shunian Chen, Ziche Liu, Feng Jiang, and Benyou Wang. Humans or llms as the judge? a study on judgement biases, 2024. URL <https://arxiv.org/abs/2402.10669>.
- [5] Xinyan Chen, Renrui Zhang, Dongzhi Jiang, Aojun Zhou, Shilin Yan, Weifeng Lin, and Hongsheng Li. Mint-cot: Enabling interleaved visual tokens in mathematical chain-of-thought reasoning. *arXiv preprint arXiv:2506.05331*, 2025.
- [6] Elias Frantar and Dan Alistarh. SparseGPT: Massive language models can be accurately pruned in one-shot. In *ICML*, 2023.
- [7] Gemma Team, Google DeepMind. Gemma 3: Open models for responsible AI. Technical report, 2025.
- [8] Aaron Grattafiori, Abhimanyu Dubey, Abhinav Jauhri, Abhinav Pandey, Abhishek Kadian, Ahmad Al-Dahle, Aiesha Letman, Akhil Mathur, Alan Schelten, Alex Vaughan, Amy Yang, Angela Fan, Anirudh Goyal, Anthony Hartshorn, Aobo Yang, Archi Mitra, Archie Sravankumar, Artem Korenev, Arthur Hinsvark, Arun Rao, Aston Zhang, Aurelien Rodriguez, Austen Gregerson, Ava Spataru, Baptiste Roziere, Bethany Biron, Binh Tang, Bobbie Chern, Charlotte Caucheteux, Chaya Nayak, Chloe Bi, Chris Marra, Chris McConnell, Christian Keller, Christophe Touret, Chunyang Wu, Corinne Wong, Cristian Canton Ferrer, Cyrus Nikolaidis, Damien Allonsius, Daniel Song, Danielle Pintz, Danny Livshits, Danny Wyatt, David Esiobu, Dhruv Choudhary, Dhruv Mahajan, Diego Garcia-Olano, Diego Perino, Dieuwke Hupkes, Egor Lakomkin, Ehab AlBadawy, Elina Lobanova, Emily Dinan, Eric Michael Smith, Filip Radenovic, Francisco Guzmán, Frank Zhang, Gabriel Synnaeve, Gabrielle Lee, Georgia Lewis Anderson, Govind Thattai, Graeme Nail, Gregoire Mialon, Guan Pang, Guillem Cucurell, Hailey Nguyen, Hannah Korevaar, Hu Xu, Hugo Touvron, Iliyan Zarov, Imanol Arrieta Ibarra, Isabel Kloumann, Ishan Misra, Ivan Evtimov, Jack Zhang, Jade Copet, Jaewon Lee, Jan Geffert, Jana Vranes, Jason Park, Jay Mahadeokar, Jeet Shah, Jelmer van der Linde, Jennifer Billock, Jenny Hong, Jenya Lee, Jeremy Fu, Jianfeng Chi, Jianyu Huang, Jiawen Liu, Jie Wang, Jiecao Yu, Joanna Bitton, Joe Spisak, Jongsoo Park, Joseph Rocca, Joshua Johnstun, Joshua Saxe, Junteng Jia, Kalyan Vasuden Alwala, Karthik Prasad, Kartikeya Upasani, Kate Plawiak, Ke Li, Kenneth Heafield, Kevin Stone, Khalid El-Arini, Krithika Iyer, Kshitiz Malik, Kuenley Chiu, Kunal Bhalla, Kushal Lakhotia, Lauren Rantala-Yeary, Laurens van der Maaten, Lawrence Chen, Liang Tan, Liz Jenkins, Louis Martin, Lovish Madaan, Lubo Malo, Lukas Blecher, Lukas Landzaat, Luke de Oliveira, Madeline Muzzi, Mahesh Pasupuleti, Mannat Singh, Manohar Paluri, Marcin Kardas, Maria Tsimpoukelli, Mathew Oldham, Mathieu Rita, Maya Pavlova, Melanie Kam-badur, Mike Lewis, Min Si, Mitesh Kumar Singh, Mona Hassan, Naman Goyal, Narjes Torabi, Nikolay Bashlykov, Nikolay Bogoychev, Niladri Chatterji, Ning Zhang, Olivier Duchenne, Onur Çelebi, Patrick Alrassy, Pengchuan Zhang, Pengwei Li, Petar Vasic, Peter Weng, Prajjwal Bhargava, Pratik Dubal, Praveen Krishnan, Punit Singh Koura, Puxin Xu, Qing He, Qingxiao

Dong, Ragavan Srinivasan, Raj Ganapathy, Ramon Calderer, Ricardo Silveira Cabral, Robert Stojnic, Roberta Raileanu, Rohan Maheswari, Rohit Girdhar, Rohit Patel, Romain Sauvestre, Ronnie Polidoro, Roshan Sumbaly, Ross Taylor, Ruan Silva, Rui Hou, Rui Wang, Saghar Hosseini, Sahana Chennabasappa, Sanjay Singh, Sean Bell, Seohyun Sonia Kim, Sergey Edunov, Shaoliang Nie, Sharan Narang, Sharath Rapparthi, Sheng Shen, Shengye Wan, Shruti Bhosale, Shun Zhang, Simon Vandenhende, Soumya Batra, Spencer Whitman, Sten Sootla, Stephane Collot, Suchin Gururangan, Sydney Borodinsky, Tamar Herman, Tara Fowler, Tarek Sheasha, Thomas Georgiou, Thomas Scialom, Tobias Speckbacher, Todor Mihaylov, Tong Xiao, Ujjwal Karn, Vedanuj Goswami, Vibhor Gupta, Vignesh Ramanathan, Viktor Kerkez, Vincent Gonguet, Virginie Do, Vish Vogeti, Vitor Albiero, Vladan Petrovic, Weiwei Chu, Wenhan Xiong, Wenyin Fu, Whitney Meers, Xavier Martinet, Xiaodong Wang, Xiaofang Wang, Xiaoqing Ellen Tan, Xide Xia, Xinfeng Xie, Xuchao Jia, Xuwei Wang, Yaelle Goldschlag, Yashesh Gaur, Yasmine Babaei, Yi Wen, Yiwen Song, Yuchen Zhang, Yue Li, Yuning Mao, Zacharie Delpierre Coudert, Zheng Yan, Zhengxing Chen, Zoe Papakipos, Aaditya Singh, Aayushi Srivastava, Abha Jain, Adam Kelsey, Adam Shajnfeld, Adithya Gangidi, Adolfo Victoria, Ahuva Goldstand, Ajay Menon, Ajay Sharma, Alex Boesenberg, Alexei Baevski, Allie Feinstein, Amanda Kallet, Amit Sangani, Amos Teo, Anam Yunus, Andrei Lupu, Andres Alvarado, Andrew Caples, Andrew Gu, Andrew Ho, Andrew Poulton, Andrew Ryan, Ankit Ramchandani, Annie Dong, Annie Franco, Anuj Goyal, Aparajita Saraf, Arkabandhu Chowdhury, Ashley Gabriel, Ashwin Bharambe, Assaf Eisenman, Azadeh Yazdan, Beau James, Ben Maurer, Benjamin Leonhardi, Bernie Huang, Beth Loyd, Beto De Paola, Bhargavi Paranjape, Bing Liu, Bo Wu, Boyu Ni, Braden Hancock, Bram Wasti, Brandon Spence, Brani Stojkovic, Brian Gamido, Britt Montalvo, Carl Parker, Carly Burton, Catalina Mejia, Ce Liu, Changhan Wang, Changkyu Kim, Chao Zhou, Chester Hu, Ching-Hsiang Chu, Chris Cai, Chris Tindal, Christoph Feichtenhofer, Cynthia Gao, Damon Civin, Dana Beaty, Daniel Kreymer, Daniel Li, David Adkins, David Xu, Davide Testuggine, Delia David, Devi Parikh, Diana Liskovich, Didem Foss, Dingkan Wang, Duc Le, Dustin Holland, Edward Dowling, Eissa Jamil, Elaine Montgomery, Eleonora Presani, Emily Hahn, Emily Wood, Eric-Tuan Le, Erik Brinkman, Esteban Arcaute, Evan Dunbar, Evan Smothers, Fei Sun, Felix Kreuk, Feng Tian, Filippos Kokkinos, Firat Ozgenel, Francesco Caggioni, Frank Nayat, Frank Seide, Gabriela Medina Florez, Gabriella Schwarz, Gada Badeer, Georgia Sweet, Gil Halpern, Grant Herman, Grigory Sizov, Guangyi, Zhang, Guna Lakshminarayanan, Hakan Inan, Hamid Shojanazeri, Han Zou, Hannah Wang, Hanwen Zha, Haroun Habeeb, Harrison Rudolph, Helen Suk, Henry Aspegren, Hunter Goldman, Hongyuan Zhan, Ibrahim Damlaj, Igor Molybog, Igor Tufanov, Ilias Leontiadis, Irina-Elena Veliche, Itai Gat, Jake Weissman, James Geboski, James Kohli, Janice Lam, Japhet Asher, Jean-Baptiste Gaya, Jeff Marcus, Jeff Tang, Jennifer Chan, Jenny Zhen, Jeremy Reizenstein, Jeremy Teboul, Jessica Zhong, Jian Jin, Jingyi Yang, Joe Cummings, Jon Carvill, Jon Shepard, Jonathan McPhie, Jonathan Torres, Josh Ginsburg, Junjie Wang, Kai Wu, Kam Hou U, Karan Saxena, Kartikay Khandelwal, Katayoun Zand, Kathy Matosich, Kaushik Veeraraghavan, Kelly Michelena, Keqian Li, Kiran Jagadeesh, Kun Huang, Kunal Chawla, Kyle Huang, Lailin Chen, Lakshya Garg, Lavender A, Leandro Silva, Lee Bell, Lei Zhang, Liangpeng Guo, Licheng Yu, Liron Moshkovich, Luca Wehrstedt, Madian Khabza, Manav Avalani, Manish Bhatt, Martynas Mankus, Matan Hasson, Matthew Lennie, Matthias Reso, Maxim Groshev, Maxim Naumov, Maya Lathi, Meghan Keneally, Miao Liu, Michael L. Seltzer, Michal Valko, Michelle Restrepo, Mihir Patel, Mik Vyatskov, Mikayel Samvelyan, Mike Clark, Mike Macey, Mike Wang, Miquel Jubert Hermoso, Mo Metanat, Mohammad Rastegari, Munish Bansal, Nandhini Santhanam, Natascha Parks, Natasha White, Navyata Bawa, Nayan Singhal, Nick Egebo, Nicolas Usunier, Nikhil Mehta, Nikolay Pavlovich Laptev, Ning Dong, Norman Cheng, Oleg Chernoguz, Olivia Hart, Omkar Salpekar, Ozlem Kalinli, Parkin Kent, Parth Parekh, Paul Saab, Pavan Balaji, Pedro Rittner, Philip Bontrager, Pierre Roux, Piotr Dollar, Polina Zvyagina, Prashant Ratanchandani, Pritish Yuvraj, Qian Liang, Rachad Alao, Rachel Rodriguez, Rafi Ayub, Raghotham Murthy, Raghu Nayani, Rahul Mitra, Rangaprabhu Parthasarathy, Raymond Li, Rebekkah Hogan, Robin Battey, Rocky Wang, Russ Howes, Ruty Rinott, Sachin Mehta, Sachin Siby, Sai Jayesh Bondu, Samyak Datta, Sara Chugh, Sara Hunt, Sargun Dhillon, Sasha Sidorov, Satadru Pan, Saurabh Mahajan, Saurabh Verma, Seiji Yamamoto, Sharadh Ramaswamy, Shaun Lindsay, Shaun Lindsay, Sheng Feng, Shenghao Lin, Shengxin Cindy Zha, Shishir Patil, Shiva Shankar, Shuqiang Zhang, Shuqiang Zhang, Sinong Wang, Sneha Agarwal, Soji Sajuyigbe, Soumith Chintala, Stephanie Max, Stephen Chen, Steve Kehoe, Steve Satterfield, Sudarshan Govindaprasad, Sumit Gupta, Summer Deng, Sungmin Cho, Sunny Virk, Suraj Subramanian, Sy Choudhury, Sydney Goldman, Tal Remez,

- Tamar Glaser, Tamara Best, Thilo Koehler, Thomas Robinson, Tianhe Li, Tianjun Zhang, Tim Matthews, Timothy Chou, Tzook Shaked, Varun Vontimitta, Victoria Ajayi, Victoria Montanez, Vijai Mohan, Vinay Satish Kumar, Vishal Mangla, Vlad Ionescu, Vlad Poenaru, Vlad Tiberiu Mihailescu, Vladimir Ivanov, Wei Li, Wenchen Wang, Wenwen Jiang, Wes Bouaziz, Will Constable, Xiaocheng Tang, Xiaojian Wu, Xiaolan Wang, Xilun Wu, Xinbo Gao, Yaniv Kleinman, Yanjun Chen, Ye Hu, Ye Jia, Ye Qi, Yenda Li, Yilin Zhang, Ying Zhang, Yossi Adi, Youngjin Nam, Yu, Wang, Yu Zhao, Yuchen Hao, Yundi Qian, Yunlu Li, Yuze He, Zach Rait, Zachary DeVito, Zef Rosnbrick, Zhaoduo Wen, Zhenyu Yang, Zhiwei Zhao, and Zhiyu Ma. The llama 3 herd of models, 2024. URL <https://arxiv.org/abs/2407.21783>.
- [9] Arthur Gretton, Karsten M. Borgwardt, Malte Rasch, Bernhard Schölkopf, and Alexander J. Smola. A kernel method for the two-sample problem. In *NeurIPS*, 2006.
- [10] Arthur Gretton, Karsten M. Borgwardt, Malte J. Rasch, Bernhard Schölkopf, and Alexander Smola. A kernel two-sample test. *Journal of Machine Learning Research*, 13:723–773, 2012.
- [11] Song Han, Jeff Pool, John Tung, and William J. Dally. Learning both weights and connections for efficient neural networks. In *NeurIPS*, 2015.
- [12] Babak Hassibi, David G. Stork, and Gregory J. Wolff. Optimal brain surgeon and general network pruning. In *IEEE International Conference on Neural Networks*, 1993.
- [13] Geoffrey Hinton, Oriol Vinyals, and Jeff Dean. Distilling the knowledge in a neural network. *arXiv preprint arXiv:1503.02531*, 2015.
- [14] Cheng-Yu Hsieh, Chun-Liang Li, Chih-Kuan Yeh, Hootan Nakhost, Yasuhisa Fujii, Alexander Ratner, Ranjay Krishna, Chen-Yu Lee, and Tomas Pfister. Distilling step-by-step! outperforming larger language models with less training data and smaller model sizes. *arXiv preprint arXiv:2305.02301*, 2023.
- [15] Kai Huang, Hao Zou, Ye Xi, BoChen Wang, Zhen Xie, and Liang Yu. IVTP: Instruction-guided visual token pruning for large vision-language models. In *ECCV*, 2024.
- [16] Kushal Kafle and Christopher Kanan. An analysis of visual question answering algorithms. In *ICCV*, 2017.
- [17] Bo-Kyeong Kim, Geonmin Kim, Tae-Ho Kim, Thibault Castells, Shinkook Choi, Junho Shin, and Hyoung-Kyu Song. Shortened llama: Depth pruning for large language models with comparison of retraining methods, 2024. URL <https://arxiv.org/abs/2402.02834>.
- [18] Minsu Kim, Jiwan Chung, et al. TAMP: Token-adaptive layerwise pruning in multimodal large language models. *arXiv preprint arXiv:2504.09897*, 2025.
- [19] Takeshi Kojima, Shixiang Shane Gu, Machel Reid, Yutaka Matsuo, and Yusuke Iwasawa. Large language models are zero-shot reasoners. In *NeurIPS*, 2022.
- [20] Tamera Lanham, Anna Chen, Ansh Radhakrishnan, Benoit Steiner, Carson Denison, Danny Hernandez, Dustin Li, Esin Durmus, Evan Hubinger, Jackson Kernion, Kamilė Lukošiuūtė, Karina Nguyen, Newton Cheng, Nicholas Joseph, Nicholas Schiefer, Oliver Rausch, Robin Larson, Sam McCandlish, Sandipan Kundu, Saurav Kadavath, Shannon Yang, Thomas Henighan, Timothy Maxwell, Timothy Telleen-Lawton, Tristan Hume, Zac Hatfield-Dodds, Jared Kaplan, Jan Brauner, Samuel R. Bowman, and Ethan Perez. Measuring faithfulness in chain-of-thought reasoning, 2023. URL <https://arxiv.org/abs/2307.13702>.
- [21] Yann LeCun, John S. Denker, and Sara A. Solla. Optimal brain damage. In *NeurIPS*, 1989.
- [22] Jaeho Lee, Sejun Park, Sangwoo Mo, Sungsoo Ahn, and Jinwoo Shin. Layer-adaptive sparsity for the magnitude-based pruning. *arXiv preprint arXiv:2010.07611*, 2021.
- [23] Bo Li, Yuanhan Zhang, et al. LLaVA-OneVision: Easy visual task transfer. *arXiv preprint arXiv:2408.03326*, 2024.
- [24] Pan Lu, Swaroop Mishra, et al. Learn to explain: Multimodal reasoning via thought chains for science question answering. In *NeurIPS*, 2022.

- [25] Qing Lyu, Shreya Havaldar, Adam Stein, Li Zhang, Delip Rao, Eric Wong, Marianna Apidianaki, and Chris Callison-Burch. Faithful chain-of-thought reasoning. In Jong C. Park, Yuki Arase, Baotian Hu, Wei Lu, Derry Wijaya, Ayu Purwarianti, and Adila Alfa Krisnadhi, editors, *Proceedings of the 13th International Joint Conference on Natural Language Processing and the 3rd Conference of the Asia-Pacific Chapter of the Association for Computational Linguistics (Volume 1: Long Papers)*, pages 305–329, Nusa Dua, Bali, November 2023. Association for Computational Linguistics. doi: 10.18653/v1/2023.ijcnlp-main.20. URL <https://aclanthology.org/2023.ijcnlp-main.20/>.
- [26] Xinyin Ma, Gongfan Fang, and Xinchao Wang. LLM-Pruner: On the structural pruning of large language models. In *NeurIPS*, 2023.
- [27] Xinyin Ma, Gongfan Fang, and Xinchao Wang. LLM-Pruner: Support for GQA and Llama-3. <https://github.com/horseee/LLM-Pruner>, 2024.
- [28] Kenneth Marino, Mohammad Rastegari, Ali Farhadi, and Roozbeh Mottaghi. OK-VQA: A visual question answering benchmark requiring external knowledge. In *CVPR*, 2019.
- [29] Silvano Martello and Paolo Toth. Knapsack problems: Algorithms and computer implementations. *Wiley*, 1990.
- [30] Paul Michel, Omer Levy, and Graham Neubig. Are sixteen heads really better than one? In *NeurIPS*, 2019.
- [31] Pavlo Molchanov, Stephen Tyree, Tero Karras, Timo Aila, and Jan Kautz. Pruning convolutional neural networks for resource efficient inference. In *ICLR*, 2017.
- [32] Pavlo Molchanov, Arun Mallya, Stephen Tyree, Iuri Frosio, and Jan Kautz. Importance estimation for neural network pruning. In *CVPR*, 2019.
- [33] Qwen Team. Qwen2-VL: Enhancing vision-language model’s perception of the world at any resolution. Technical report, 2024.
- [34] Qwen Team. Qwen2.5-VL: Technical report. Technical report, 2025.
- [35] Dustin Schwenk, Apoorv Khandelwal, Christopher Clark, Kenneth Marino, and Roozbeh Mottaghi. A-OKVQA: A benchmark for visual question answering using world knowledge. In *ECCV*, 2022.
- [36] Hao Shao, Shengju Qian, Han Xiao, Guanglu Song, Zhuofan Zong, Letian Wang, Yu Liu, and Hongsheng Li. Visual cot: Advancing multi-modal language models with a comprehensive dataset and benchmark for chain-of-thought reasoning. *Advances in Neural Information Processing Systems*, 37:8612–8642, 2024.
- [37] Noam Shazeer. Glu variants improve transformer, 2020. URL <https://arxiv.org/abs/2002.05202>.
- [38] Mingjie Sun, Zhuang Liu, Anna Bair, and J. Zico Kolter. A simple and effective pruning approach for large language models. In *ICLR*, 2024.
- [39] Yi-Lin Sung, Jaehong Yoon, and Mohit Bansal. ECoFLaP: Efficient coarse-to-fine layer-wise pruning for vision-language models. In *ICLR*, 2024.
- [40] Naftali Tishby, Fernando C. Pereira, and William Bialek. The information bottleneck method. *arXiv preprint physics/0004057*, 2000.
- [41] Elena Voita, David Talbot, Fedor Moiseev, Rico Sennrich, and Ivan Titov. Analyzing multi-head self-attention: Specialized heads do the heavy lifting, the rest can be pruned. In *ACL*, 2019.
- [42] Hanzhang Wang, Jiawen Zhang, and Qingyuan Ma. Exploring intrinsic dimension for vision-language model pruning. In *ICML*, 2024.
- [43] Jason Wei, Xuezhi Wang, Dale Schuurmans, Maarten Bosma, Fei Xia, Ed Chi, Quoc V Le, Denny Zhou, et al. Chain-of-thought prompting elicits reasoning in large language models. *Advances in neural information processing systems*, 35:24824–24837, 2022.

- [44] Nakyeong Yang, Yunah Jang, Hwanhee Lee, Seohyeong Jeong, and Kyomin Jung. Task-specific compression for multi-task language models using attribution-based pruning. In *Findings of EACL*, 2023.
- [45] Zhengyuan Yang, Linjie Li, Jianfeng Wang, Kevin Lin, Ehsan Azarnasab, Faisal Ahmed, Zicheng Liu, Ce Liu, Michael Zeng, and Lijuan Wang. Mm-react: Prompting chatgpt for multimodal reasoning and action. *arXiv preprint arXiv:2303.11381*, 2023.
- [46] Xubing Ye, Yukang Gan, Yixiao Ge, Xiao-Ping Zhang, and Yansong Tang. ATP-LLaVA: Adaptive token pruning for large vision language models. In *arXiv preprint arXiv:2412.00447*, 2024.
- [47] Lu Yin, You Wu, Zhenyu Zhang, et al. Outlier weighed layerwise sparsity (OWL): A missing secret sauce for pruning LLMs to high sparsity. In *ICML*, 2024.
- [48] Xuan Zhang, Chao Du, Tianyu Pang, Qian Liu, Wei Gao, and Min Lin. Chain of preference optimization: Improving chain-of-thought reasoning in LLMs. In *NeurIPS*, 2024.
- [49] Zhuosheng Zhang, Aston Zhang, Mu Li, Hai Zhao, George Karypis, and Alex Smola. Multimodal chain-of-thought reasoning in language models. *arXiv preprint arXiv:2302.00923*, 2023.
- [50] Zhuosheng Zhang, Aston Zhang, Mu Li, et al. Multimodal chain-of-thought reasoning in language models. In *ACL*, 2023.
- [51] Lianmin Zheng, Wei-Lin Chiang, Ying Sheng, Siyuan Zhuang, Zhanghao Wu, Yonghao Zhuang, Zi Lin, Zhuohan Li, Dacheng Li, Eric P. Xing, Hao Zhang, Joseph E. Gonzalez, and Ion Stoica. Judging llm-as-a-judge with mt-bench and chatbot arena, 2023. URL <https://arxiv.org/abs/2306.05685>.
- [52] Michael Zhu and Suyog Gupta. To prune, or not to prune: Exploring the efficacy of pruning for model compression. *arXiv preprint arXiv:1710.01878*, 2017.

A Ablation studies

A.1 μ CRASP: Is each component necessary?

We systematically ablate each component of μ CRASP on Qwen2.5-VL-7B at 50% pruning, an aggressive regime that exposes the contribution of each mechanism.

Table A: Component ablation on Qwen2.5-VL-7B at 50% pruning. Each row removes one component from the full μ CRASP framework, where J stands for LLM-Judge score, EM_a for string exact match of final Answer, SEM_{c+a} for Semantic Similarity (cosine) of the complete $CoT + final\ answer$, Fmt for Formatting Score which measures if the model can generate step-by-step formatted reasoning steps

Variant	Physical				Quantitative				Commonsense			
	J	EM_a	SEM_{c+a}	Fmt	J	EM_a	SEM_{c+a}	Fmt	J	EM_a	SEM_{c+a}	Fmt
Full μ CRASP	7.43	38.0	69.9	26.5	6.02	23.0	78.0	21.0	6.15	7.0	73.4	20.6
– Pivot ($\gamma=0$)	6.81	25.8	67.2	16.5	5.85	13.5	79.9	23.0	5.54	5.9	71.4	21.7
– CMDS ($\beta=0$)	6.09	27.3	51.1	21.8	5.10	17.5	78.5	24.4	5.79	6.3	71.6	17.2

(1) **Pivot attribution drives answer precision on grounded reasoning.** We removed the pivot signal ($\gamma_{dyn}=0$) that drops LLM-J by 0.62 points on Physical (7.43 \rightarrow 6.81) and 6.02 on Commonsense (6.02 \rightarrow 5.85), with EM_a falling by 32% points on Physical (38.0 \rightarrow 25.8) and 41% on Quantitative (23.0 \rightarrow 13.5). The mechanism’s impact scales with how tightly reasoning steps depend on visual grounding: Physical reasoning requires the model to chain observations (“I see a white shirt”) into conclusions (“Therefore the lead player wears white”), and pivot tokens at these transitions carry the cross-modal signal. Commonsense reasoning, which relies somewhat on distributed knowledge, shows the smallest LLM-J drop (0.61 points).

(2) **CMDS protection is essential for cross-modal integrity.** Removing CMDS ($\beta=0$) produces the steepest SEM_{c+a} drop in the entire ablation: Physical crashes from 69.9 to 51.1 (–27%), indicating severe disruption of vision-language alignment. LLM-J falls from 7.43 to 6.09 (–1.34 points) and Formatting Score from 26.5 to 21.8. Without CMDS, the pruner distributes cuts uniformly across layers, removing units in the vision-language fusion band (layers 11 – 18) that the sliding window ablation (Fig 3(b)) identifies as the cross-modal bottleneck. On Commonsense, the SEM_{c+a} and LLM-J drops are smaller (1.8 and 0.36 LLM-J points respectively), consistent with these domains relying less on visual grounding.

(3) **Random pivots confirm that pivot location matters, not just pivot existence.** We replaced real pivot tokens with randomly selected positions provides a critical control: if μ CRASP’s gains came merely from restricting the attribution window to *any* token subset, random pivots should perform comparably. Table B shows they do not.

Table B: Random vs. real pivot selection on Qwen2.5-VL-7B at 50% pruning. Random pivots recover only partial gains over no-pivot, confirming that correct identification of reasoning transitions drives μ CRASP’s advantage where J stands for LLM-Judge score, EM_a for string exact match of final Answer, SEM_{c+a} for Semantic Similarity (cosine) of the complete $CoT + final\ answer$, Fmt for Formatting Score which measures if the model can generate step-by-step formatted reasoning steps

Pivot Selection	Physical				Quantitative				Commonsense			
	J	EM_a	SEM_{c+a}	Fmt	J	EM_a	SEM_{c+a}	Fmt	J	EM_a	SEM_{c+a}	Fmt
No Pivot ($\gamma=0$)	7.13	25.8	67.2	16.5	6.02	13.5	79.9	23.0	5.54	5.9	71.4	21.7
Random Pivot	6.95	29.2	73.1	17.8	5.79	11.9	78.6	22.5	5.53	6.0	72.0	20.8
Real Pivot (default)	7.85	38.0	69.9	26.5	6.36	23.0	78.0	21.0	6.15	7.0	73.4	20.6

Random pivots recover EM_a only partially over the no-pivot baseline on Physical (29.2 vs 25.8, compared to 38.0 for real pivots) and actually *hurt* EM on Quantitative (11.9 vs 13.5 for no-pivot). LLM-J follows the same pattern: random pivots reach 6.95 on Physical (vs 7.85 for real, 71.3 for none) but only 5.53 on Commonsense (vs 6.15 for real, 5.54 for none), performing no better than

removing pivots entirely. The gap between random and real pivots, particularly the 8.8-point EM_a gap on Physical and 11.1-point gap on Quantitative confirms that μ CRASP’s gains come from correctly identifying reasoning-transition tokens, not from the mere act of restricting the attribution window to a subset of positions. Interestingly, random pivots achieve the highest Semantic Similarity on Physical (73.1, above both real pivots at 69.9 and no-pivot at 67.2), suggesting they preserve broad semantic content while failing to protect the specific inter-step transitions that EM_a and LLM-J measure.

A.2 Pivot Marker Taxonomy for Transition Token Detection

We detect reasoning transition tokens by scanning the generated CoT sequence for surface-level markers that signal a shift in the model’s reasoning state. These markers fall into two broad classes *structural delimiters* and *logical connectives* each targeting a different surface realisation of the same underlying event: the model completing one reasoning step and initiating the next. Structural delimiters are explicit formatting cues that CoT prompts typically encourage, such as numbered prefixes and terminal answer markers. Logical connectives are natural-language words and phrases that signal causal or conclusory transitions; they capture the same step boundaries in models whose outputs are less rigidly formatted. For each detected marker, we construct a transition window $\mathcal{M}_W = \{t : |t - i| \leq W\}$ of half-width $W=8$ tokens centered on the marker position i , and restrict the pivot attribution loss to token positions within this window (Eq. 8 in the main paper). When no marker from either class is found in a sample, approximately 15% of cases, we fall back to equal-interval partitioning of the response into three segments and treat the segment boundaries as pivot positions. Table C provides the complete taxonomy of markers used in our implementation, together with representative examples drawn from generated CoT traces. The taxonomy is intentionally broad so that it generalizes to CoT formats produced by different models and prompting conventions; adding or removing individual patterns has negligible effect on results, as the random-pivot ablation in App. B confirms.

A.3 Global allocation is indispensable.

We replaced global knapsack allocation with uniform layerwise pruning, where every layer receives the same pruning ratio, causes the most catastrophic failure across all ablations (Table D).

LLM-J collapses from 7.43 to 4.40 on Physical (−3.30 points), from 6.02 to 3.85 on Quantitative (−2.13), and from 6.15 to 3.85 on Commonsense (−2.30). EM drops to the lowest across all domains (3.03, 2.2, 3.01) and Formatting Score falls to ~ 1.5 , indicating that the pruned model can barely produce coherent CoT structure. Layerwise allocation forces equal pruning ratios on every layer, which removes a disproportionate number of cheap MLP neurons in some layers while under-pruning expensive GQA groups in others, a particularly destructive mismatch given the $\sim 250\times$ per-unit cost disparity in Qwen2.5-VL-7B (5.2M parameters per GQA group vs 21K per MLP neuron), $\sim 85\times$ in Gemma 3 4B (0.66M vs 7.7K), and $\sim 21\times$ in Qwen2-VL-2B (98K vs 4.6K). This ablation delivered us the strongest reason for the global knapsack formulation: even with pivot attribution and CMDS protection intact, layerwise allocation renders the model non-functional. The knapsack solver allows the pruner to concentrate its budget on high-value, high-CMDS layers while aggressively compressing low-importance regions, a flexibility that uniform allocation fundamentally cannot provide.

A.4 Transition window size exhibits a clear optimum at $W=8$.

Table E compares three window sizes. Both $W=4$ and $W=16$ degrade performance relative to $W=8$, but through different mechanisms.

Table E: Effect of transition window size W on Qwen2.5-VL-7B at 50% pruning.

W	Physical				Quantitative				Commonsense			
	J	EM_a	SEM_{c+a}	Fmt	J	EM_a	SEM_{c+a}	Fmt	J	EM_a	SEM_{c+a}	Fmt
$W=4$	7.70	27.4	75.7	19.9	6.0	11.4	78.1	31.8	5.84	6.6	73.6	21.9
$W=8$ (default)	7.85	38.0	69.9	26.5	6.36	23.0	78.0	21.0	6.15	7.0	73.4	20.6
$W=16$	7.72	30.5	67.2	23.9	5.60	6.7	77.2	21.9	5.59	7.0	71.4	20.6

Table C: Taxonomy of pivot markers used for reasoning transition token detection. Markers in both classes are matched case-insensitively via regular expressions. The window \mathcal{M}_W of half-width $W=8$ is constructed around each detected position.

Class	Sub-type	Patterns (regex)	Example in CoT trace
Structural Delimiters	Numbered step	<code>^(\d+)[.])\s</code>	1. I observe a red ball...
	Labelled step	<code>Step\s*\d+\s*[:-]</code>	Step 2: The object is circular...
	Sub-step	<code>(\d+)(\d+)\s</code>	1.1 Examining the left panel...
	Final answer	<code>Final Answer[:-]</code>	Final Answer: three
	Answer marker	<code>\bAnswer\b\s*[:-]</code>	Answer: blue
	Conclusion label	<code>(Conclusion Summary)[:-]</code>	Conclusion: the taller object...
	Think/reason tag	<code><think> </think></code>	</think> The answer is four.
Logical Connectives	Causal conclusion	<code>\b(Therefore Thus Hence)\b</code>	Therefore, the count is two.
	Consequence	<code>\b(So Consequently As a result)\b</code>	So the glass will spill over.
	Inference	<code>\b(This means This implies This suggests)\b</code>	This means the car is moving left.
	Deduction	<code>\b(We can (therefore thus) conclude)\b</code>	We can therefore conclude that...
	Summary	<code>\b(In (summary conclusion) To summarize)\b</code>	In summary, three forks are visible.
	Transition adverb	<code>\b(Next Now Moving on Finally)\b</code>	Next, I identify the spatial layout.
	Contrastive pivot	<code>\b(However Nevertheless Despite this)\b</code>	However, the shadow indicates depth.
Additive reasoning	<code>\b(Furthermore Additionally Moreover)\b</code>	Furthermore, the label reads "exit".	
Fallback (no marker found)		Equal-interval partition	Response split into 3 equal segments; boundaries treated as pivots.

$W=4$ captures too few context tokens around each pivot, reducing the signal-to-noise ratio of the attribution score: EM_a drops by 11% on Physical and 12% on Quantitative relative to $W=8$. $W=16$ dilutes the pivot signal by including too many non-transition tokens, collapsing toward global attribution: Quantitative EM_a drops from 23.0 to 6.7 (-16.3) and LLM-J from 6.36 to 5.60, while Commonsense LLM-J falls from 6.15 to 3.85. An instructive counter-pattern appears in Semantic Similarity, which *peaks* at $W=4$ on Physical (75.7 vs 69.9 for $W=8$): the narrower window preserves overall semantic content, responses remain topically relevant, but sacrifices the precise inter-step transitions that EM_a and LLM-J measure. This dissociation reinforces that embedding similarity alone is insufficient for evaluating CoT preservation. The default $W=8$ achieves the best EM_a and LLM-J across all three domains, striking the optimal balance between capturing sufficient transition context and maintaining pivot specificity.

Table D: Global vs. layerwise allocation on Qwen2.5-VL-7B at 50% pruning. Layerwise allocation collapses reasoning across all domains despite retaining the same total parameter count, where J stands for LLM-Judge score, EM_a for string exact match of final Answer, SEM_{c+a} for Semantic Similarity (cosine) of the complete *CoT + final answer*, Fmt for Formatting Score which measures if the model can generate step-by-step formatted reasoning steps

Allocation	Physical				Quantitative				Commonsense			
	J	EM_a	SEM_{c+a}	Fmt	J	EM_a	SEM_{c+a}	Fmt	J	EM_a	SEM_{c+a}	Fmt
Global (default)	7.43	38.0	69.9	26.5	6.02	23.0	78.0	21.0	6.15	7.0	73.4	20.6
Layerwise	4.40	3.03	66.2	1.5	3.89	2.2	62.1	4.1	3.85	3.01	57.3	10.8

A.5 Output Distribution Fidelity: Logit Divergence Analysis

Standard evaluation metrics such as LLM-Judge, Exact Match, and Semantic Similarity operate on *generated text* and therefore capture downstream effects of pruning only after auto-regressive decoding amplifies or dampens initial distortions. To measure how faithfully each pruning method preserves the dense model’s predictive behaviour at the source, we compute per-token KL divergence directly on the output logit distributions across all three reasoning domains.

Setup. We feed 512 image–question–CoT samples from each domain’s calibration set through both the dense (unpruned) Qwen2.5-VL-7B and each pruned variant at 30% ratio. At every answer-token position (i.e., positions where the training label is not masked), we extract the full-vocabulary logit vector, convert it to a probability distribution via softmax, and compute $D_{KL}(p_{\text{dense}}||p_{\text{pruned}})$. We restrict the computation to answer tokens because these carry the reasoning and final-answer content; prompt and image tokens are excluded. Token positions that produce NaN or infinite KL values due to numerical edge cases in softmax are filtered out; fewer than 0.1% of positions are affected. The resulting per-token KL distributions are shown in Fig 4 for all three domains.

Results. Table F reports mean KL divergence per method on the Physical domain; the Commonsense and Quantity panels in Fig 4 show near-identical distributional structure. μ CRASP achieves a mean of 0.92 nats per token on Physical reasoning, representing a $1.66\times$ reduction over LLM-Pruner (1.53), a $3.6\times$ reduction over Wanda-SP (3.31), a $4.5\times$ reduction over FLAP (4.11), and an $11.4\times$ reduction over Attribution Pruning (10.51).

Table F: Mean per-token KL divergence ($D_{KL}(\text{dense}||\text{pruned})$) on Qwen2.5-VL-7B at 30% pruning, Physical domain. The Commonsense and Quantity domains yield near-identical rankings (Fig 4).

Method	Mean KL (nats)	Ratio vs. μ CRASP
μ CRASP	0.92	1.0 \times
LLM-Pruner	1.53	1.7 \times
Wanda-SP	3.31	3.6 \times
FLAP	4.11	4.5 \times
Attribution Pruning	10.51	11.4 \times

Domain-consistency of distributional fidelity. The most important observation from Fig 4 is that the relative ordering and distributional shapes are essentially invariant across all three domains. In every panel, μ CRASP’s KL density concentrates sharply near zero (peak density ~ 0.80), while Attribution Pruning produces a broad bimodal distribution centered near 10–11 nats with substantial mass extending past 15 nats. LLM-Pruner consistently sits closest to μ CRASP but with a noticeably heavier right tail, Wanda-SP and FLAP occupy intermediate positions, and their cross-domain ordering is preserved. This domain-invariance directly parallels the domain-agnostic LLM-J gains reported in Section 6: the same architectural structures that μ CRASP protects via CMDS and pivot attribution are the ones responsible for logit-level fidelity regardless of reasoning type.

Connection to reasoning preservation. In auto-regressive generation, each token’s probability distribution conditions all subsequent predictions. When pruning distorts the logit distribution at a given position, the error compounds through the remaining sequence: the model selects a different

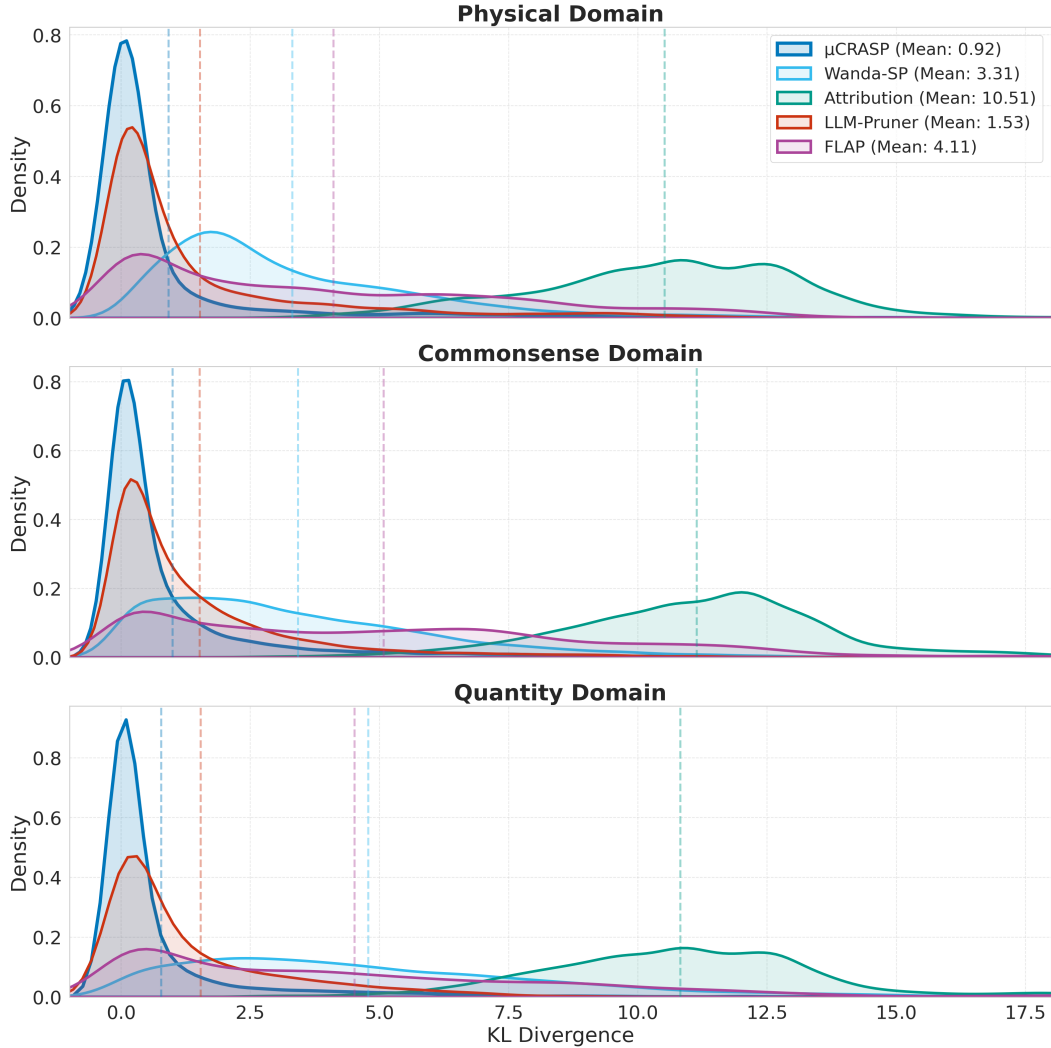


Figure 4: Per-token KL divergence distributions ($D_{\text{KL}}(\text{dense}||\text{pruned})$) on Qwen2.5-VL-7B at 45% pruning across all three reasoning domains. Dashed vertical lines mark per-method means. μCRASP concentrates KL mass near zero (mean 0.92 nats) in every domain, while baselines exhibit broader and right-shifted distributions. The near-identical distributional structure across Physical, Commonsense, and Quantity confirms that μCRASP 's output fidelity is domain-agnostic.

token, which shifts the context for the next prediction, producing a cascading deviation from the dense model's reasoning trajectory. μCRASP 's low and tightly concentrated KL divergence ensures that the pruned model's token-by-token decisions remain closely aligned with the dense model's across all three domains, preventing the cascading errors that cause baselines to produce logically incoherent reasoning chains despite generating fluent text. This observation complements the pivot attribution analysis (Section 7): pivot tokens at reasoning-step boundaries are precisely the positions where even small logit distortions redirect the entire downstream reasoning trajectory, and μCRASP 's concentrated low-KL profile protects these critical positions most effectively and does so consistently whether the task demands visual grounding, numerical precision, or world knowledge.

B μ CRASP Algorithm

Algorithm 1 μ CRASP: Modality-and-Reasoning-Aware Global Knapsack Pruning for VLMs

Require: VLM \mathcal{M} , Calibration Set \mathcal{D} , Pruning Ratio S , γ_{base} , ρ , Window W , Pivot Extractor Φ_{pivot}

Ensure: Pruned VLM \mathcal{M}'

```

1: % Phase 1: Global Attribution
2:  $A_{\text{global}} \leftarrow 0$ 
3: for each batch  $b \in \mathcal{D}$  do
4:   Compute  $\mathcal{L}_{\text{LM}}$ ; backpropagate;  $A_{\text{global}} \leftarrow A_{\text{global}} + |\mathcal{W} \odot \nabla_{\mathcal{W}} \mathcal{L}|$ 
5: end for
6:  $\bar{A}_{\text{global}} \leftarrow A_{\text{global}} / |\mathcal{D}|$ 
7: % Phase 2: Trajectory Pivot Attribution
8:  $A_{\text{pivot}} \leftarrow 0$ ,  $N_{\text{trans}} \leftarrow 0$ 
9: for each batch  $b \in \mathcal{D}$  do
10:   $\mathcal{I}_{\text{pivot}} \leftarrow \Phi_{\text{pivot}}(b)$ 
11:  if  $\mathcal{I}_{\text{pivot}} \neq \emptyset$  then
12:     $\mathcal{M}_W \leftarrow \bigcup_{i \in \mathcal{I}_{\text{pivot}}} \{t : |t - i| \leq W\}$ 
13:    Compute  $\mathcal{L}_{\text{pivot}}$  on  $\mathcal{M}_W$  (Eq. 6); backpropagate
14:     $A_{\text{pivot}} \leftarrow A_{\text{pivot}} + |\mathcal{W} \odot \nabla_{\mathcal{W}} \mathcal{L}_{\text{pivot}}|$ ;  $N_{\text{trans}} \leftarrow N_{\text{trans}} + 1$ 
15:  end if
16: end for
17:  $\bar{A}_{\text{pivot}} \leftarrow A_{\text{pivot}} / N_{\text{trans}}$ 
18: % Phase 3: Layer-Level Profiling
19: for each layer  $L$  do
20:   $\text{Sens}(L) \leftarrow \sqrt{\mathbb{E}[\|h_L\|_2^2]}$ ;  $\text{CMDS}(L) \leftarrow \text{Eq. 10}$ 
21: end for
22: % Phase 4: Fusion & Protection
23:  $\gamma_{\text{dyn}} \leftarrow \gamma_{\text{base}}(1 - S)^\rho$ ;  $A_{\text{fused}} \leftarrow (1 - \gamma_{\text{dyn}})\bar{A}_{\text{global}} + \gamma_{\text{dyn}}\bar{A}_{\text{pivot}}$ 
24: Compute  $\mathcal{P}(L)$  for all layers (Eq. 13)
25: % Phase 5: Knapsack Packing
26: for each unit  $u$  do
27:   $E_u \leftarrow A_{\text{fused}}^{(u)} \times \mathcal{P}(L_u) / c(u)$ 
28: end for
29: Sort by  $E_u$ ; greedily pack into  $\mathcal{K}$  until  $\sum c(u) \leq (1 - S) \times \text{TotalParams}$ 
30: % Phase 6: Safety Enforcement
31: Override  $\mathcal{K}$  to satisfy min-retention (Eq. 15);  $\mathcal{M}' \leftarrow \text{PhysicalPrune}(\mathcal{M}, \mathcal{K})$ 
32: return  $\mathcal{M}'$ 

```

B.1 Global Attribution Scoring

In autoregressive generation, a response $Y = (y_1, \dots, y_T)$ is produced token-by-token. Aggregating the first-order Taylor importance $\Delta \mathcal{L} \approx \mathbf{w}_u^\top \nabla_{\mathbf{w}_u} \mathcal{L}$ over all token positions yields the global score:

$$I_{\text{global}}(u) = \sum_{t=1}^T \left| \mathbf{w}_u^\top \nabla_{\mathbf{w}_u} \ell(y_t \mid y_{<t}) \right|, \quad (2)$$

accumulated over the calibration dataset \mathcal{D} .

For **MLP units**, pruning neuron j removes its parameters across gate, up, and down projections. Its importance aggregates across all three:

$$I_{\text{global}}^{\text{MLP}}(j) = \sum_{\text{proj} \in \{g, u, d\}} \sum_k \left| W_{\text{proj}}^{jk} \cdot \frac{\partial \mathcal{L}}{\partial W_{\text{proj}}^{jk}} \right|. \quad (3)$$

For **attention units**, let \mathcal{H}_u denote the parameter indices associated with unit u (a single head in MHA, or a positional group in GQA). Its importance is:

$$I_{\text{global}}^{\text{attn}}(u) = \sum_{d \in \mathcal{H}_u} \left(\left| W_Q^d \cdot \nabla_{W_Q^d} \mathcal{L} \right| + \left| W_O^d \cdot \nabla_{W_O^d} \mathcal{L} \right| \right). \quad (4)$$

B.2 Trajectory Pivot Attribution

Equation 2 aggregates importance uniformly across all T token positions, which is suboptimal for CoT reasoning. Instead, CoT generation can be viewed as a trajectory over latent reasoning states $Z = (z_1, \dots, z_K)$, where most tokens describe intermediate states with predictable structure, while a small subset corresponds to transitions between reasoning steps. These transition tokens are sparse ($\sim 5\%$ of the sequence) yet disproportionately informative for reasoning progression, and their contribution is diluted under global aggregation.

Transition region estimation. We model CoT as a sequence of state transitions: $p(y | x) = \prod_{k=1}^K p(z_k | z_{<k}, x) \cdot p(a | z_{1:K}, x)$. Each conditional $p(z_k | z_{<k}, x)$ is governed by localized regions where the model transitions between reasoning states. Rather than assuming a fixed format, we estimate a set of transition indices $\mathcal{I}_{\text{pivot}}$ as a coarse approximation to these boundaries.

In practice, we identify candidate transitions using lightweight structural cues when available (e.g., step delimiters or discourse shifts), and otherwise fall back to uniform segmentation of the sequence. This procedure is not intended to be exact, but to provide a weak localization of transition regions that is agnostic to specific CoT formats.

Around each estimated transition, we construct a local window:

$$\mathcal{M}_W = \bigcup_{i \in \mathcal{I}_{\text{pivot}}} \{t : |t - i| \leq W\}, \quad (5)$$

which captures the tokens most relevant for reasoning state updates. As shown in our ablations, the effectiveness of this approach does not depend on precise boundary identification, but rather on concentrating attribution around transition regions.

Pivot attribution score. We restrict the loss to transition tokens:

$$\mathcal{L}_{\text{pivot}} = - \sum_{t \in \mathcal{M}_W} \log p_{\theta}(y_t | y_{<t}, x^v, x^t), \quad (6)$$

and compute first-order Taylor importance on this restricted loss, normalized by the number of pivots:

$$A_{\text{pivot}}(u) = \frac{1}{|\mathcal{I}_{\text{pivot}}|} \sum_{t \in \mathcal{M}_W} |\mathbf{w}_u^{\top} \nabla_{\mathbf{w}_u} \ell(y_t | y_{<t})|. \quad (7)$$

Trajectory Pivot Attribution can be interpreted as a conditional variant of Taylor-based importance estimation [32], where the loss landscape is restricted to transition tokens. This aligns with information-theoretic perspectives on compression: effective pruning should preserve components that retain high mutual information with future reasoning states while discarding those that merely decode low-entropy syntactic patterns [40].

Pivot extraction serves as a proxy for latent reasoning state transitions. While explicit markers make these boundaries observable, the underlying assumption is that reasoning trajectories contain sparse transition points irrespective of surface form. In principle, pivot identification can be replaced with more general boundary detection methods (e.g., entropy peaks, attention shifts, or learned segmentation), making the approach applicable beyond explicitly structured CoT traces.

B.3 Cross-Modal Dependency Score (CMDSD)

Existing pruning methods do not explicitly account for cross-modal interactions between vision and language tokens. They may remove components critical for aligning visual and textual representations, leading to degraded multimodal reasoning. We seek a principled measure that quantifies how strongly a layer differentiates between modalities.

Distributional formulation. We formulate cross-modal dependency as a divergence between vision and text token activation distributions. Let \mathbb{P}_V and \mathbb{P}_T denote these distributions at layer L . We quantify their discrepancy through Maximum Mean Discrepancy (MMD) [10, 9], a kernel-based two-sample test:

$$\text{MMD}[\mathcal{H}, \mathbb{P}_V, \mathbb{P}_T] = \sup_{\|f\|_{\mathcal{H}} \leq 1} (\mathbb{E}_{h_v}[f(h_v)] - \mathbb{E}_{h_t}[f(h_t)]). \quad (8)$$

MMD equals zero if and only if $\mathbb{P}_V = \mathbb{P}_T$ for characteristic kernels [10]. We instantiate with a linear kernel $\kappa(x, y) = x^\top y$, yielding a tractable estimate:

$$\text{MMD}_L = \|\mathbb{E}[h_v] - \mathbb{E}[h_t]\|_2. \quad (9)$$

To obtain a scale-invariant measure, we normalize by the expected activation magnitude:

$$\text{CMDS}(L) = \frac{\left\| \mathbb{E}[\text{Act}_{\text{vis}}^{(L)}] - \mathbb{E}[\text{Act}_{\text{txt}}^{(L)}] \right\|_2}{\mathbb{E} \left[\|\text{Act}_{\text{all}}^{(L)}\|_2 \right] + \epsilon}. \quad (10)$$

High CMDS values indicate strong modality-specific transformations (critical cross-modal integration), while low values correspond to modality-agnostic processing. Empirically, CMDS peaks in middle layers across all four VLMs we evaluate (Fig.3).

B.4 Layer Output Sensitivity

Second-order pruning methods estimate importance using curvature information (e.g., inverse Hessian) [12, 6], but are computationally infeasible for large VLMs. We adopt a lightweight proxy based on forward perturbation in the Transformer residual stream.

In a Transformer, each layer contributes additively: $x_{\ell+1} = x_\ell + f_\ell(x_\ell)$. Pruning units in layer L perturbs its output h_L , introducing an error δ_L that propagates through subsequent layers. The magnitude of δ_L scales with $\|h_L\|_2$, implying that layers producing larger activations are more sensitive to pruning. Moreover, LayerNorm does not fully absorb such perturbations: it normalizes the full vector, so a large δ_L changes the *relative* feature magnitudes even after normalization. We define layer sensitivity as:

$$\text{Sens}(L) = \sqrt{\mathbb{E}_{x \sim \mathcal{D}} [\|h_L(x)\|_2^2]}, \quad (11)$$

where $h_L(x)$ is the output of layer L 's output projection (down_proj for MLP, o_proj for attention). $\text{Sens}(L)$ serves as a zeroth-order proxy for the structural load carried by a layer.

B.5 Dynamic Gamma Fusion and Global Knapsack

Pruning Ratio-Conditioned Score Fusion. Since Trajectory Pivot Attribution ($A_{\text{pivot}}^{(u)}$) and global attribution ($I_{\text{global}}^{(u)}$) capture complementary aspects of importance, we fuse their scores in a way, that is adaptive to the pruning ratio regime: reasoning structure is more critical at low ratio, while core token prediction dominates under tighter budgets. The fused importance is:

$$A_{\text{fused}}^{(u)} = (1 - \gamma_{\text{dyn}}) \cdot \bar{A}_{\text{global}}^{(u)} + \gamma_{\text{dyn}} \cdot \bar{A}_{\text{pivot}}^{(u)}, \quad (12)$$

where $\bar{A}_{\text{global}}^{(u)}$ and $\bar{A}_{\text{pivot}}^{(u)}$ are normalized importance scores. We model the trade-off via a pruning ratio-conditioned mixing coefficient: $\gamma_{\text{dyn}}(S) = \gamma_{\text{base}} \cdot (1 - S)^\rho$, which smoothly decreases the contribution of the reasoning-specific signal as pruning ratio increases.

Layer-Level Protection Factors. To account for cross-layer variation in structural importance, we introduce a multiplicative protection factor:

$$\mathcal{P}(L) = (1 + \alpha \cdot \widetilde{\text{Sens}}(L)) \cdot (1 + \beta \cdot \widetilde{\text{CMDS}}(L)) \cdot \Omega(L), \quad (13)$$

where $\widetilde{\text{Sens}}$ and $\widetilde{\text{CMDS}}$ are normalized sensitivity and cross-modal dependency scores.

The structural prior $\Omega(L)$ captures position- and module-specific importance, reflecting empirical observations that certain layers (e.g., early, late, and attention-heavy layers) are more sensitive to pruning. The coefficients α and β scale with pruning ratio, enabling stronger differentiation under tighter parameter budgets. Full specification is in Table K.

B.5.1 Global Knapsack Formulation

We cast pruning as a global resource allocation problem. Each unit u has value $v(u) = A_{\text{fused}}^{(u)} \cdot \mathcal{P}(L_u)$ and cost $c(u)$, under budget $\mathcal{C}_{\text{target}} = \text{TotalParams} \cdot (1 - S)$. The objective is:

$$\max_{\mathcal{K} \subseteq \bigcup_\ell \mathcal{U}_\ell} \sum_{u \in \mathcal{K}} v(u) \quad \text{subject to} \quad \sum_{u \in \mathcal{K}} c(u) \leq \mathcal{C}_{\text{target}}. \quad (14)$$

We solve this via greedy efficiency ranking $E_u = v(u)/c(u)$, packing units until the budget is exhausted. To prevent degenerate solutions, we enforce minimum retention:

$$|\mathcal{K} \cap \mathcal{U}_L| \geq \eta_L, \quad (15)$$

where η_L is a pruning ratio-dependent threshold. Structured pruning removes weight matrix rows/columns, yielding a smaller dense model. The complete algorithm is in Algorithm B.

C Failure of Magnitude Pruning in VLMs

We observe that magnitude-based pruning exhibits catastrophic degradation when applied to VLMs, even at low pruning levels. While the unpruned model maintains reasonable performance (e.g., LLM-J ≈ 69.7 , PPL ≈ 2.21), pruning rapidly leads to complete collapse of reasoning behavior. At pruning levels as low as 20–30%, EM_a drops to 0, formatting consistency collapses, and perplexity increases by several orders of magnitude (e.g., $> 10^3$ to $> 10^5$), indicating loss of coherent generation.

This behavior is consistent across models and domains, and reflects a fundamental limitation of magnitude pruning: it is agnostic to both task structure and cross-modal dependencies, leading to removal of units critical for maintaining reasoning coherence. Due to this extreme scale mismatch and degenerate outputs, magnitude pruning results are not directly comparable to other methods in the main plots and are therefore reported separately here for completeness.

Table G: Representative results of magnitude pruning on Qwen2.5-VL-3B (Commonsense). The method exhibits rapid collapse with increasing pruning level.

Levels	EM_a	EM_{c+a}	PPL	Formatting
0%	39.65	81.98	2.21	99.87
20%	0.00	14.28	1.97×10^3	0.00
30%	0.00	10.00	1.46×10^5	0.00
40%	0.00	11.30	4.41×10^5	0.00

D Datasets

We evaluate μ CRASP across four benchmarks spanning distinct reasoning domains. Each dataset was selected to test a different facet of multimodal reasoning that pruning must preserve: commonsense inference, quantitative computation, physical attribute recognition.

A-OKVQA (Commonsense Reasoning). A-OKVQA [35] is a crowdsourced benchmark of approximately 25K questions over COCO images that require commonsense and world knowledge to answer. Unlike earlier knowledge-based VQA datasets such as OK-VQA [28], A-OKVQA questions generally cannot be answered by querying a knowledge base and instead require multi-step reasoning grounded in the visual scene. We use the official train/validation split and evaluate on the validation set. This dataset serves as our primary benchmark for commonsense reasoning, as the questions naturally elicit multi-step CoT responses.

TDIUC-Quantitative (Quantitative Reasoning). To evaluate quantitative reasoning (counting, numerical comparison, and arithmetic inference), we construct a targeted subset from the TDIUC dataset [16], which organizes VQA into 12 semantically distinct task categories to enable fine-grained analysis of reasoning capabilities. TDIUC explicitly includes counting and numerical reasoning tasks, making it well-suited for our evaluation.

We extract quantitative questions via a multi-stage filtering pipeline designed to balance precision and scalability. First, we apply keyword-based filtering (e.g., “how many”, “how much”, “number of”) to obtain a high-recall candidate pool. Second, we employ a strong LLM-based verifier GPT-4o to classify whether each question requires explicit numerical reasoning, filtering out cases solvable via simple object recognition or memorization.

To assess annotation quality, we perform human validation on a randomly sampled subset (20%) of the filtered data. The human annotator verifies whether the retained questions genuinely require

quantitative reasoning, enabling estimation of the classifier precision and correction of systematic errors.

TDIUC-Physical (Physical Reasoning). To evaluate physical attribute reasoning (e.g., color, shape, size, material, and spatial configuration), we construct a dedicated subset from the TDIUC dataset [16], which provides fine-grained task categorization for visual question answering.

We extract physical reasoning questions using a multi-stage filtering pipeline designed to balance coverage and precision. First, we apply keyword-based filtering (e.g., “what color”, “what shape”, “how big”, “what material”) to obtain a high-recall candidate pool. Second, we employ a strong LLM-based verifier (GPT-4o) to classify whether each question genuinely requires reasoning about physical properties, filtering out cases solvable via simple label retrieval or direct object recognition. GPT-4o is a high-capacity multimodal model capable of reasoning across visual and textual inputs, making it well-suited for this verification step.

To assess annotation quality, we perform human validation on a randomly sampled subset (20%) of the filtered data. Annotators verify whether each question requires reasoning about physical attributes under a consistent labeling protocol. This allows us to estimate the precision of the automated pipeline and identify systematic errors.

Both of this semi-automated pipeline follows common practice in large-scale dataset curation, combining heuristic filtering with model-based verification and human auditing to ensure both scalability and quality. While keyword filtering may introduce noise and LLM-based verification may inherit model biases, the human-in-the-loop evaluation provides a quantitative estimate of reliability, and our analysis shows that residual noise does not affect the comparative evaluation across pruning methods.

Dataset statistics. Table H summarizes the key statistics of all four benchmarks.

Table H: Dataset statistics

Dataset	Domain	Train	Val	Test	Source
A-OKVQA	Commonsense	17.1K	1.1K	6.7K	COCO
TDIUC-Quant.	Quantitative	15K	2K	3.56K	TDIUC
TDIUC-Physical	Physical	15K	2K	3K	TDIUC

E Baselines

We compare μ CRASP against four baselines that span the major paradigms in structured pruning. All baselines are adapted to perform *structural* pruning (removing entire neurons, attention heads, or GQA groups) to ensure a fair comparison with our method, which also produces dense sub-networks. We focus exclusively on structural pruning baselines, as unstructured methods (e.g., SparseGPT [6]) produce irregular sparsity patterns that do not yield practical inference speedup without specialized hardware, whereas our goal is to produce smaller dense models deployable on commodity hardware.

(1) Magnitude Pruning. The simplest structured pruning baseline removes structural units (neurons or attention groups) with the smallest aggregate ℓ_1 weight norm [11, 52]. For each MLP neuron j , we compute $\sum_k |W_{\text{gate}}^{jk}| + |W_{\text{up}}^{jk}| + |W_{\text{down}}^{kj}|$; for each attention unit, we aggregate across Q and O projection slices. Units are ranked globally and the lowest-scoring ones are removed until the target pruning ratio is reached.

(2) Attribution-Based Pruning. Following Yang et al. [44], we use an attribution method to determine which neurons are essential for performing the target task. This approach computes task-specific attribution scores using gradient-based saliency and prunes units with low attribution. Unlike the Taylor score baseline, which uses a single global loss, attribution-based pruning explicitly conditions importance on the downstream task distribution, providing a stronger baseline for task-aware compression.

(3) LLM-Pruner. LLM-Pruner [26] discovers coupled structures via dependency graphs and estimates group importance using a combination of first-order and second-order Taylor approximations. It then performs structural pruning by removing entire dependency groups and recovers performance via LoRA fine-tuning. LLM-Pruner now supports GQA architectures [27], making it directly applicable to our Qwen-family models. We use the official implementation with default hyperparameters and `param_second` importance estimation. Since, we are evaluating one-shot pruning performance without any recovery phase, for this baseline we didn’t apply the LORA-recovery phase.

(4) FLAP. FLAP [2] introduces a fluctuation-based structured pruning criterion that evaluates whether the output feature map is easily recoverable when a column of weight is removed. It standardizes importance scores to adaptively determine the global compressed model structure, and adds bias terms to compensate for removed neurons. FLAP also provides a structured adaptation of the Wanda criterion, which we use as our Wanda baseline. We use the official implementation with default settings.

(5) Wanda (Structural). Following the structured Wanda variant introduced by An et al. [2] (denoted Wanda-sp in their paper), we adapt the Wanda pruning criterion [38] from unstructured to structural pruning. For each structural unit, importance is computed as the product of the unit’s weight magnitude and the L_2 norm of its corresponding input activations, aggregated across all dimensions of the unit. This provides a gradient-free, computationally efficient baseline.

Baseline implementation notes. All baselines use the same calibration set of 128 samples, the same target pruning ratio levels, and the same evaluation protocol as μ CRASP.

F Synthetic CoT Generation

Our method requires CoT-annotated calibration data, i.e., image-question pairs accompanied by multi-step reasoning traces. Since the target VLMs (2B–7B parameters) do not reliably produce high-quality CoT traces at their native scale, we use a larger teacher model to generate synthetic annotations.

Teacher model. We use GPT-4o as the CoT generator. We chose this model for three practical reasons. First, it is a strong, readily available vision-language model with reliable instruction-following behavior. Second, it produces consistent and well-structured reasoning traces, which is important for extracting trajectory-level signals. Finally, GPT-4o is architecturally different from the target models used in our experiments (e.g., Qwen, Gemma), which helps reduce potential bias arising from using the same model family for both data generation and evaluation.

Generation protocol. For each image-question pair in the calibration set, we prompt the teacher model with the following system instruction:

Prompt for CoT Generation

You are a helpful AI assistant that solves visual questions with clear step-by-step reasoning. For each example, you will be provided with the following information:

1. Image
2. Question
3. Answer (if the answer is incorrect, ignore it and generate the correct answer based on the image and question)

Please generate a reasoning chain with 2–3 concise steps where needed, referencing specific visual cues (“I observe...”, “Because I see...”), then provide the final answer.

Format:

Step-by-Step Thought:

1. I observe ...
2. I infer ...
3. Therefore ...

deduced_answer: {final_answer}

Constraints:

- Since this is a quantitative reasoning question, write numbers in words (e.g., “one”, “two”)

We generate CoT traces using greedy decoding (temperature = 0) to ensure reproducibility. To ensure annotation quality, all generated CoT traces were manually reviewed by two human annotators, including one of the authors. The review process verified that the reasoning traces were logically consistent, grounded in the visual content, and aligned with the final answer. Traces containing incomplete reasoning, hallucinated visual evidence, or inconsistent conclusions were discarded and regenerated. This additional verification step ensured that the entire dataset including the calibration set contained reliable reasoning trajectories suitable for pruning analysis.

Calibration set construction. From the training split of each dataset, we randomly sample 128 image-question pairs and pair them with their corresponding synthetic CoT traces. This calibration set is used for all scoring phases (global attribution, trajectory pivot attribution, CMDS, and sensitivity profiling). The same calibration set is used across all baselines to ensure fair comparison.

G Experimental Settings

G.1 Hardware

All pruning and evaluation has been carried out in NVIDIA A40 46GB GPUs including the scoring phase of μ CRASP (global attribution, trajectory pivot attribution, CMDS, and sensitivity profiling) are all done using 2 * 46 GB (A40 Chips). And, for full finetuning of the models with CoT Traces we used NVIDIA H100 GPUs.

All evaluation (inference on validation sets, perplexity computation, metric calculation) and baseline pruning methods are also executed the same GPUs. Table I summarizes the hardware allocation.

Table I: Hardware allocation across experimental stages.

Stage	Hardware	Approx. Time
Finetuning (7B model)	2 * H100 80GB	~ 4 Hr
Pruning (7B model)	2 * A40 46GB	~ 45 min
Metrics Evaluation	2 * A40 46GB	~ 30 min

Table J: Architecture comparison of evaluated vision-language models. We report the number of vision encoder and language decoder layers, attention type, vision backbone, and multimodal fusion strategy.

Model	Enc (Vision)	Dec (LM)	Attention	Vision Backbone	Fusion
Qwen2-VL 2B	32	28	GQA	Qwen2 ViT	Patch merger
Qwen2.5-VL 3B	32	36	GQA	Qwen2.5 ViT	Patch merger
Qwen2.5-VL 7B	32	28	GQA	Qwen2.5 ViT	Patch merger
Gemma 3 4B	27	34	GQA	SigLIP ViT	AvgPool projector

G.2 Architecture Details

We evaluate a diverse set of recent vision-language models spanning the Qwen2-VL and Gemma 3 families. All models follow a modular design consisting of a vision encoder, a language decoder, and a lightweight multimodal fusion mechanism. The Qwen-based models employ a ViT-style vision backbone with 3D patch embeddings and an MLP-based patch merger for modality alignment. In contrast, Gemma models utilize a SigLIP-based vision encoder combined with a pooling-based projection module. Across all models, the language component adopts grouped-query attention (GQA) for efficient decoding. Table J summarizes the key architectural differences.

G.3 Hyperparameters

Table K provides the complete hyperparameter specification for μ CRASP.

Table K: Complete hyperparameter settings for μ CRASP.

Component	Parameter	Value
Trajectory Pivot	Window W	8
	Min. steps for detection	2
	Fallback segmentation	Equal thirds
Dynamic Gamma	γ_{base}	0.4
	Decay ρ	2
Layer Protection	Sensitivity coeff. α	$0.3 + 1.5S$
	CMDS coeff. β	$0.2 + S$
Position Protection	Early layers N_E	4
	Final layers N_F	2
	Early boost	$1 + 0.5(1 - \ell/N_E)$
	Final boost	1.3
Structure Protection	Attention boost ω	1.8
	Vision boost ω	1.2
Safety Constraints	Attn min keep	$\max(2, \lfloor n \cdot \max(0.35, 0.70(1-S)) \rfloor)$
	MLP min keep	$\max(1, \lfloor n \cdot \max(0.05, 0.25(1-S)) \rfloor)$
Calibration	Samples per dataset	128
	Batch size	2
	Sequence length	Model-dependent (max context)

G.4 LLM-as-Judge Protocol

Traditional evaluation metrics such as Exact Match, BLEU, ROUGE-L, or perplexity primarily measure lexical overlap or token prediction quality, but do not directly assess whether a generated chain-of-thought (CoT) trace remains logically coherent after pruning. In practice, a pruned model may still produce fluent text with reasonable semantic similarity while containing internally inconsistent reasoning steps or unsupported conclusions. To evaluate reasoning preservation more directly, we employ an LLM-as-a-Judge (LLM-J) protocol that scores the logical validity of generated CoT traces.

Judge model. We use GPT-3.5-TURBO as the evaluator model. Importantly, the judge model is distinct from both the CoT generator (GPT-4O) and the target VLMs used in our experiments, reducing potential evaluator bias toward any specific model family or architecture.

Evaluation procedure. For each evaluation sample, the judge model receives:(i) the image-question pair,(ii) the reference reasoning trace,(iii) the model-generated CoT trace, and(iv) the final predicted answer.The judge is instructed to evaluate:

- logical coherence of intermediate reasoning steps,
- consistency across reasoning transitions,
- grounding of reasoning in the visual context,
- alignment between the reasoning trace and final answer.

The judge assigns a continuous score on a 0–10 scale, where higher values indicate stronger logical validity and reasoning coherence.

Why a continuous 0–10 scale? We adopt a continuous scoring scheme instead of binary correctness labels to better capture gradual degradation in reasoning quality under pruning. Structured pruning often produces partially coherent reasoning traces that remain semantically meaningful despite containing minor logical inconsistencies or incomplete conclusions. A continuous scale therefore allows finer-grained assessment of intermediate failure modes that are not captured by discrete correctness metrics.

Likert-style interpretation. To improve interpretability, we additionally provide a Likert-style qualitative interpretation of LLM-J score ranges. This mapping serves only as an interpretation aid and does not alter the underlying quantitative evaluation used throughout the paper.

Table L: Likert-style interpretation of LLM-J scores.

LLM-J Range	Likert Level	Interpretation
0 – 2	1	Incoherent or logically invalid reasoning
2 – 4	2	Major reasoning inconsistencies
4 – 6	3	Partially coherent reasoning
6 – 8	4	Mostly coherent reasoning
8 – 10	5	Strong logical coherence and grounding

. For example, the LLM-J score of 8.87 achieved by μ CRASP on Physical reasoning at 30% pruning level corresponds to Likert level 5, indicating that the generated reasoning traces remain logically coherent and well grounded despite substantial compression.

Human verification. To verify reliability of the evaluation protocol, a subset of generated reasoning traces was manually inspected by two annotators, including one of the authors. We observed strong qualitative agreement between human judgments and LLM-J scores, particularly in distinguishing coherent reasoning from structurally collapsed outputs.

G.5 Visual Grounding and Hallucination Analysis

To further evaluate whether compressed VLMs preserve faithful visual reasoning, we perform an additional analysis of visual grounding and hallucination behavior. Beyond logical coherence, an important failure mode under aggressive pruning is the tendency to generate reasoning traces that are either weakly grounded in the image or contain hallucinated visual details unsupported by the input.

Evaluation protocol. For each sample, we provide GPT-4O with: (i) the input image, (ii) the question, (iii) the generated CoT trace, with the final predicted answer. The evaluator is instructed to assess two complementary properties:

- **Grounding Score:** measures how well the generated reasoning trace is supported by observable visual evidence in the image in the scale of 0–10.

- **Hallucination Score:** measures the extent to which the reasoning trace introduces unsupported, fabricated, or contradictory visual details also in the scale of 0–10.

μ CRASP generally preserves visually grounded reasoning even under high pruning ratio, whereas competing baselines frequently exhibit semantic drift, unsupported object descriptions, repetitive degeneration, or complete collapse into incoherent text. For example, FLAP and Wanda-SP often generate syntactically corrupted or repetitive outputs, while LLM-Pruner tends to produce fluent but weakly grounded reasoning traces that ignore critical visual evidence. Attribution-based pruning occasionally retains partial reasoning structure, but often introduces hallucinated visual attributes or incomplete conclusions under higher compression. Representative qualitative examples are provided in App.§ M.

Table M: Visual grounding and hallucination analysis at 50% pruning on the Physical domain dataset. Scores are assigned by GPT-4O on a 0–10 scale. Higher Grounding is better; lower Hallucination is better.

Method	Grounding Score \uparrow	Hallucination Score \downarrow
μ CRASP	8.6	1.8
LLM-Pruner	4.9	5.7
Wanda-SP	2.8	7.9
Attribution Pruning	5.6	4.8
FLAP	1.9	8.6

The results suggest that preserving reasoning coherence alone is insufficient; effective pruning must additionally maintain alignment between generated reasoning and visual evidence. Methods that ignore cross-modal dependencies tend to hallucinate unsupported objects, attributes, or scene interpretations as compression increases, even when the generated text remains superficially fluent.

Prompt for Visual Grounding and Hallucination Evaluation

You are an expert evaluator for vision-language reasoning systems.

You will be given:

1. An image
2. A question about the image
3. A generated chain-of-thought (CoT) reasoning trace
4. A final predicted answer

Your task is to evaluate the quality of the reasoning trace along two dimensions:

- **Grounding Score (0–10):** Evaluate how well the reasoning is supported by observable visual evidence in the image. High scores indicate that the reasoning correctly references visible objects, attributes, spatial relations, and scene details.
- **Hallucination Score (0–10):** Evaluate the extent to which the reasoning introduces fabricated, unsupported, contradictory, or irrelevant visual details. High scores indicate severe hallucination or semantic drift.

Evaluation Guidelines:

- Penalize reasoning traces that mention objects, colors, entities, or actions not visible in the image.
- Penalize repetitive, degenerate, or logically inconsistent reasoning.
- Reward concise reasoning grounded in explicit visual observations.
- Consider both the reasoning trace and the final answer jointly.

Output Format:

Grounding Score: <0-10>

Hallucination Score: <0-10>

Short Explanation: <brief justification>

H Dataset Filtering

H.1 LLM-based Verification Prompt

We use a structured prompt to classify whether a question requires quantitative reasoning. The prompt is designed to minimize ambiguity and enforce a binary decision with justification.

Prompt for Quantitative Reasoning Classification

Instruction: You are given a visual question from a VQA dataset. Determine whether answering this question requires **quantitative reasoning**, such as counting, numerical comparison, or arithmetic inference.

Definition of quantitative reasoning: A question requires quantitative reasoning if it involves:

- Counting objects (e.g., “How many cars are there?”)
- Numerical comparison (e.g., “Are there more cats than dogs?”)
- Arithmetic reasoning (e.g., “How many total items are there if we combine both groups?”)

A question does **not** require quantitative reasoning if it can be answered by:

- Simple object recognition (e.g., “What is in the image?”)
- Attribute identification (e.g., “What color is the car?”)
- Yes/No questions without counting or numerical comparison

Question:

<INSERT QUESTION HERE>

Output format:

- Label: {Quantitative / Not Quantitative}
- Justification: One sentence explaining the decision

We retain only questions classified as *Quantitative*.

H.2 Human Annotation Protocol

To validate the quality of the automatically filtered dataset, we conduct human evaluation on the entire dataset.

Annotation task. Two Annotators are presented with a question (without model prediction) and asked to determine whether it requires quantitative reasoning according to the same definition used in the LLM prompt.

Guidelines. Annotators are instructed to follow these criteria:

- Label as **Quantitative** if the answer requires counting, numerical comparison, or arithmetic reasoning.
- Label as **Not Quantitative** if the answer can be obtained via direct perception or recognition without numerical reasoning.
- In ambiguous cases, prefer the label corresponding to the *minimal reasoning required*.

Quality control. To ensure consistency:

- A subset of samples is independently annotated twice to measure inter-annotator agreement.
- Disagreements are resolved through adjudication.
- We report Cohen’s κ and raw agreement in Appendix X.

Error estimation. The human annotations are used to estimate:

- Precision of the LLM classifier
- Error rate of the automated filtering pipeline

Following standard human-in-the-loop annotation practices, this hybrid pipeline combines scalable model-based pre-filtering with human validation to ensure high-quality labels while maintaining efficiency.

I Discussion

Why is VLM Pruning Harder Than LLM Pruning? Indirect evidence from our cross-model results supports the claim that VLM pruning is harder than LLM pruning. On Gemma-3-4B, all baselines designed for LLMs collapse at 20-25% pruning ratio on Physical and Commonsense reasoning, despite prior work showing that 4B-parameter text-only models can sustain 30–40% unstructured pruning ratio with minimal degradation [6]. The key difference is cross-modal coupling: pruning a unit that is unimportant for text generation may be critical for routing information from the vision encoder. The catastrophic failure of LLM-Pruner on Gemma-3-4B, a method with strong reported results on text-only LLMs, is the most direct evidence for this claim.

Perplexity is a misleading proxy for reasoning quality. While most of the existing works [39, 26, 17] on pruning (Both Structured and Unstructured) benchmarked the pruned models on perplexity, we found that reasoning has little to no correlation with perplexity. For instance on Qwen2.5-VL-7B Physical at 30%, Base Taylor achieves PPL 1.59 - *lower* than μ CRASP’s 1.74 - yet its LLM-J is 13.33 versus 88.65. The pruned model generates fluent, low-surprise text that is logically incoherent that is correct tokens without correct reasoning. Conversely, when reasoning genuinely collapses (e.g., LLM-Pruner on Gemma-3-4B at 25%, LLM-J dropping from 67.71 to 5.35), the perplexity explosion to $> 10^6$ occurs only at much higher pruning ratio, long after the model is non-functional. This disconnect, observed across all model sizes, highlights that token-level metrics are insufficient for evaluating CoT preservation and motivates towards LLM-as-Judge protocol.

J Limitations.

(1) Pivot extraction relies on heuristic pattern matching for step boundary detection; learned segmentation methods could improve robustness for free-form CoT responses. (2) The protection

factor hyperparameters (α , β , N_E , N_F , attention boost) are manually chosen, though our ablations (Table 4) demonstrate robustness to individual component removal. (3) Evaluation is conducted exclusively on English-language benchmarks; multilingual CoT preservation remains unexplored. (4) LLM-as-Judge, while more informative than surface-level metrics like BLEU and F1, may itself have systematic biases that do not capture all reasoning failure modes. (5) Our experiments cover VLMs up to 7B parameters; scaling behavior on larger models (e.g., 72B) remains an open question, though prior work on LLM pruning [6] suggests that larger models are generally more amenable to compression.

K Societal Impact

Our work develops a structured pruning framework that compresses vision-language models while preserving chain-of-thought reasoning quality. The primary positive societal impact is enabling deployment of capable multimodal reasoning models on resource-constrained hardware, reducing the energy cost and carbon footprint of inference and broadening access to VLM technology beyond well-resourced institutions. On the negative side, more efficient VLMs are easier to deploy at scale, which lowers the barrier to misuse for generating disinformation, synthetic media, or automated manipulation of visual content. We do not introduce any new capability beyond what the dense model already possesses; our method only reduces the computational cost of accessing those capabilities. We do not anticipate disproportionate fairness harms specific to our pruning technique, though we acknowledge that compressed models may amplify existing biases present in the base VLM if pruning disproportionately removes parameters responsible for underrepresented concepts. We encourage practitioners deploying pruned VLMs to conduct bias audits appropriate to their application domain.

L Model Compression–Performance Curves

We provide full compression-performance curves for all evaluated VLMs across three reasoning domains (Physical, Quantitative, Commonsense) and multiple evaluation metrics. Each figure reports performance as a function of pruning ratio, comparing μ CRASP with all baselines.

These plots highlight the qualitative differences between methods: while existing pruning approaches exhibit abrupt degradation or collapse beyond moderate pruning level, μ CRASP maintains stable reasoning performance and degrades more gracefully across metrics. For clarity, each model is shown on a separate page.

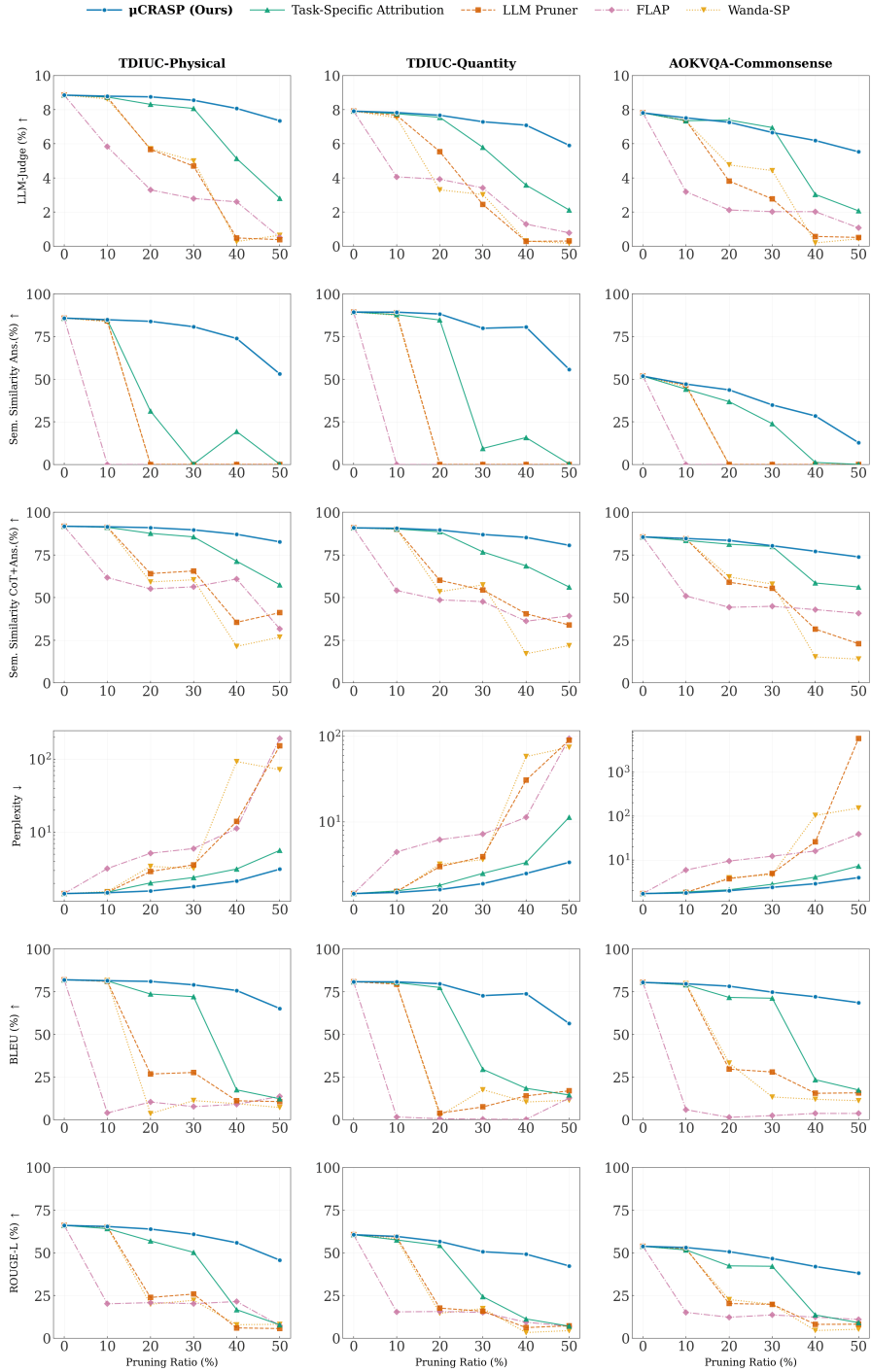


Figure 5: Compression–performance curves for LLAMA 3.2 11B across three reasoning domains. Rows correspond to different evaluation metrics, and columns correspond to domains.

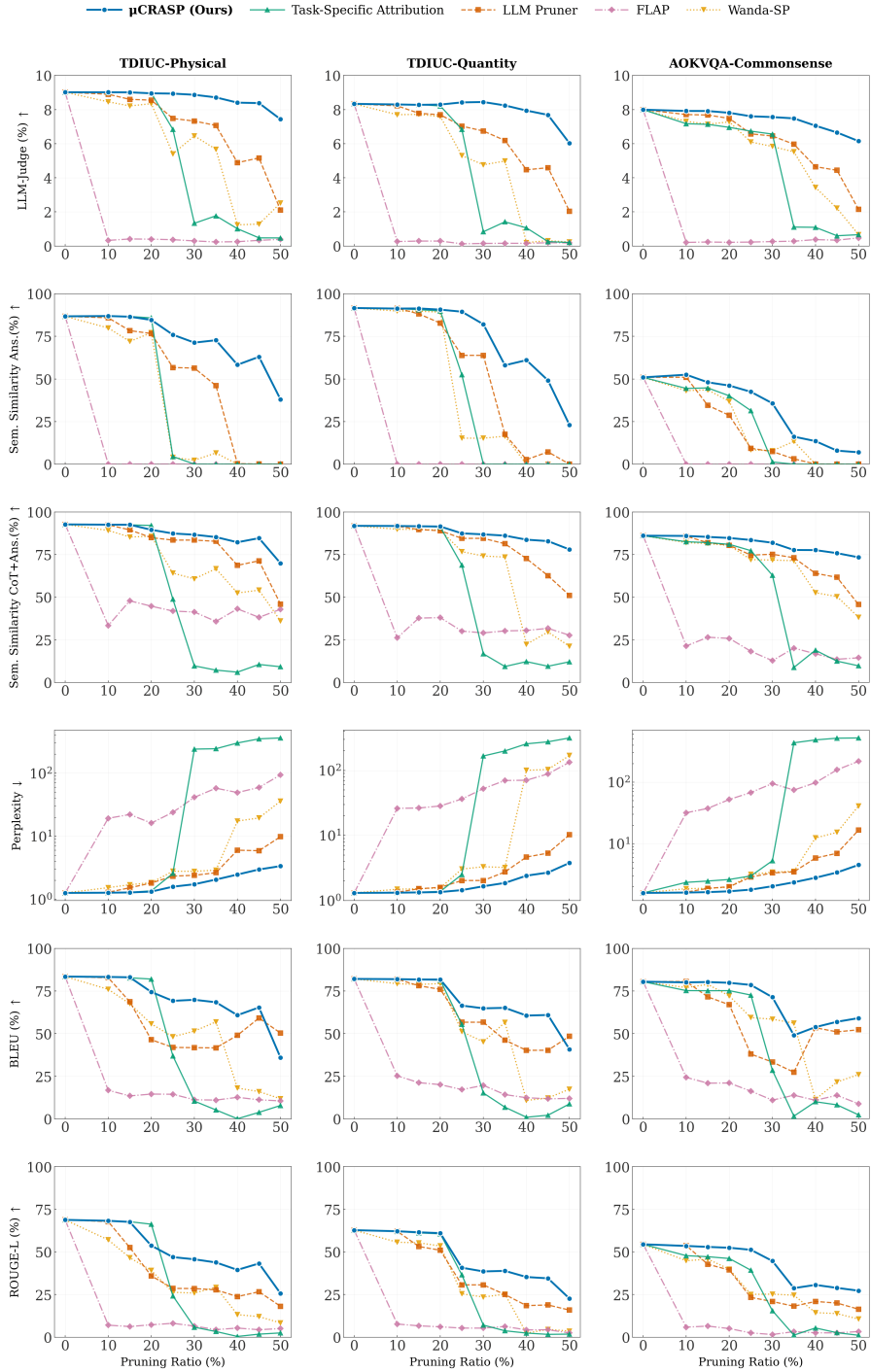


Figure 6: Compression–performance curves for Qwen2.5-VL-7B across three reasoning domains. Rows correspond to different evaluation metrics, and columns correspond to domains.

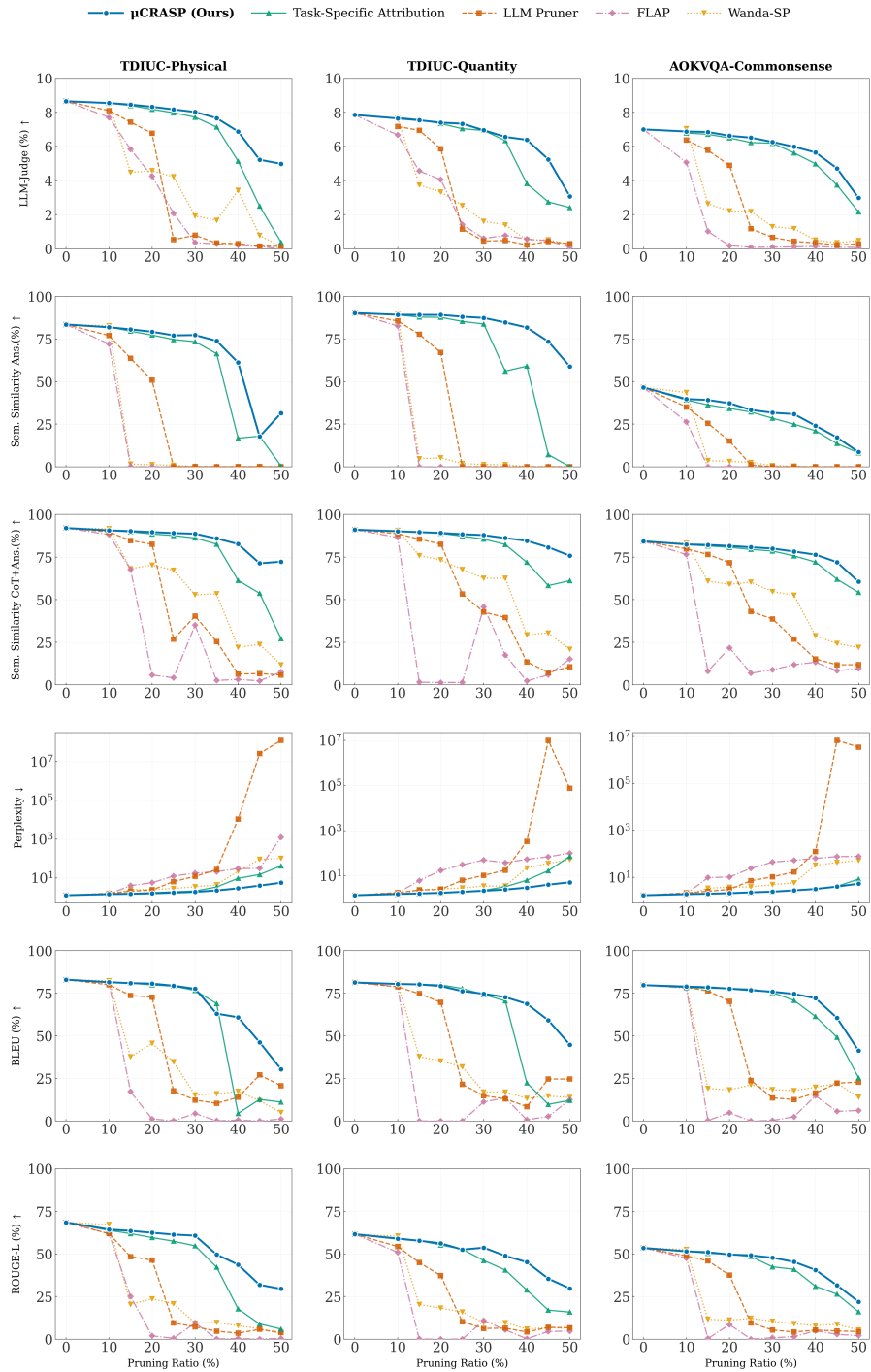


Figure 7: Compression–performance curves for Gemma-3-4B across three reasoning domains.

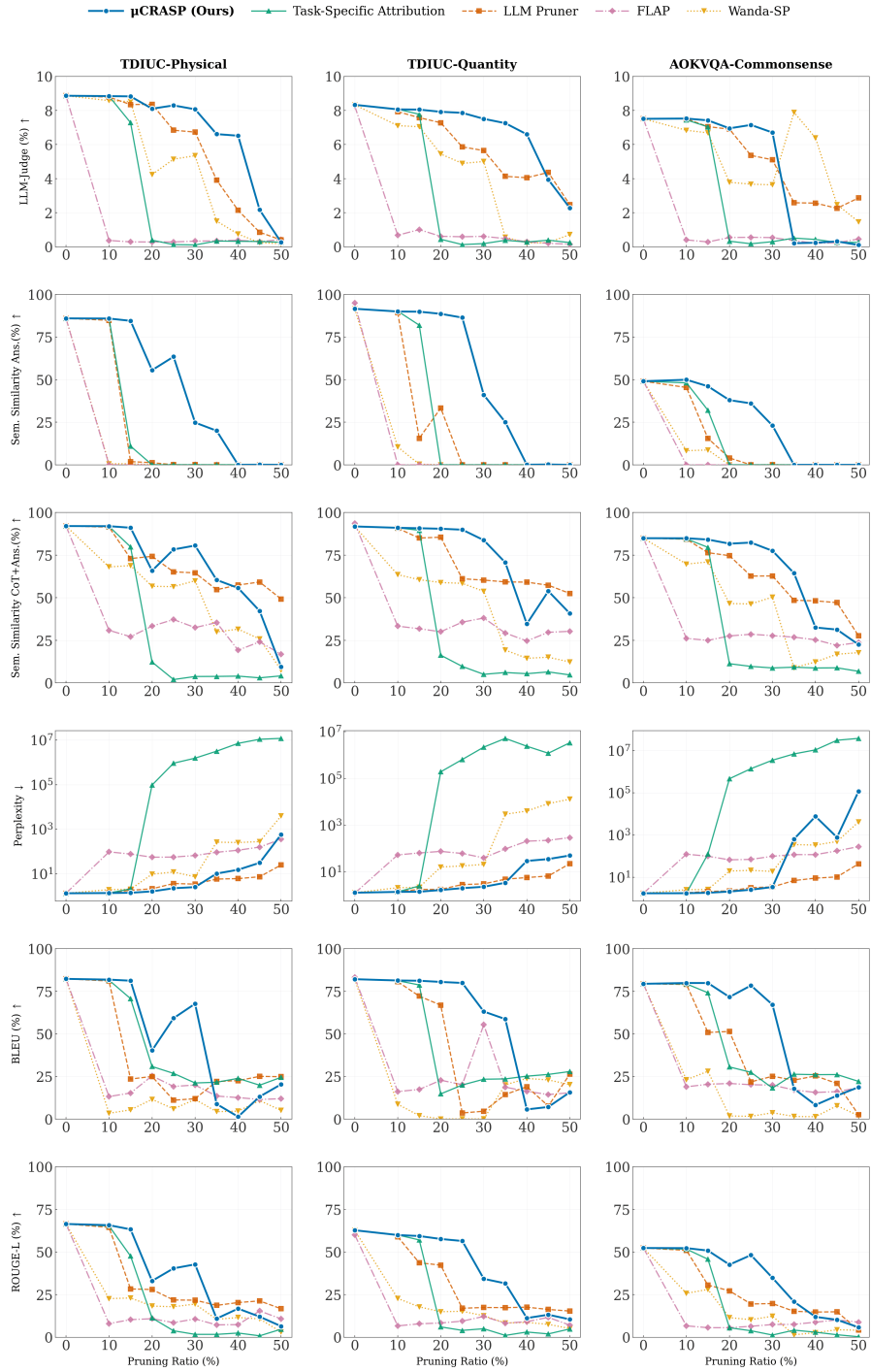


Figure 8: Compression–performance curves for Qwen2.5-VL-3B across three reasoning domains.

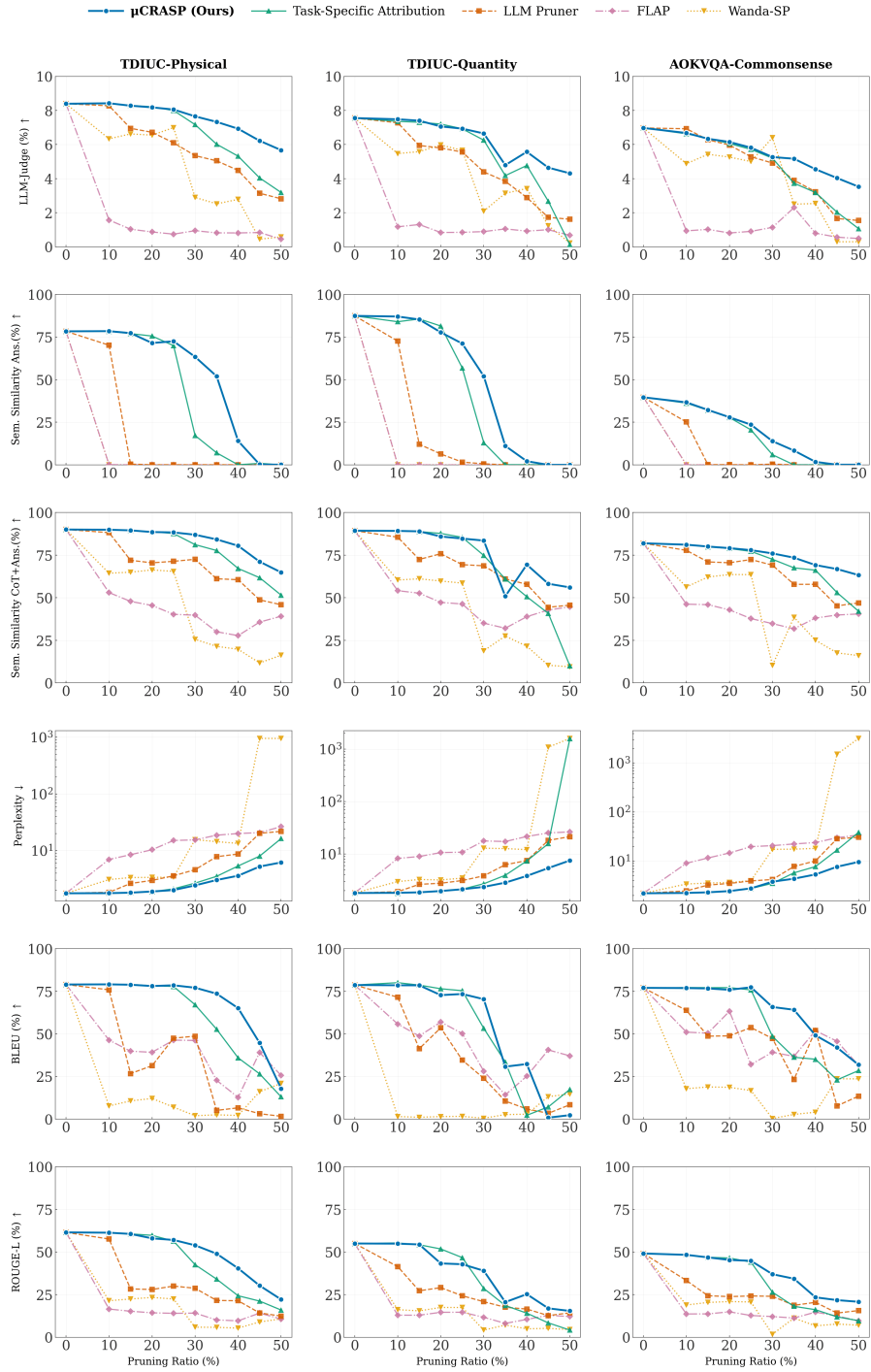


Figure 9: Compression-performance curves for Qwen2-VL-2B across three reasoning domains.


<p>Question: What is the color of the lead player's shirt?</p>	<p>FLAP: The generated response becomes fragmented and semantically incoherent, failing to correctly identify the player's shirt color. ...[truncated]</p>
	<p>LLM-Pruner: The image shows a football player in action, likely within a soccer match scenario. However, the generated response focuses on unrelated visual cues and fails to correctly determine the shirt colour of the lead player.</p>
<p>Ground Truth COT Trace: Step-by-Step Thought: 1. I observe the player in the foreground wearing a white shirt with the number "15" on it. 2. The player appears to be leading the action because they are closest to the ball and actively engaged in play. 3. Therefore, the color of the lead player's shirt is white. Final Answer: white.</p>	<p>Attribution Score: Step 1: Identify the main subject of the image. The main subjects are the soccer players actively engaged on the field. Step 2: Analyse the players' uniforms and clothing details. One player is incorrectly described as wearing a navy blue jersey paired with pink shoes and matching socks. Step 3: Deductive interpretation. The generated reasoning incorrectly associates these colours with the lead player and concludes an incorrect shirt colour. Final Answer: The lead player's shirt is navy blue.</p>
<p>μCRASP (Ours): Step-by-Step Thought: 1. Identify the lead player in the scene. 2. The lead player appears to be the individual closest to the ball. 3. The player is wearing a white shirt. Final Answer: The color of the lead player's shirt is white.</p>	<p>Wanda-SP: The generated response degenerates into repetitive and semantically corrupted football-related phrases. ...[truncated]</p>

Figure 10: Qualitative comparison of reasoning traces under structured pruning on player colour identification tasks.

M Qualitative Analysis

In this section we have put qualitative examples of the generated answers by our μ CRASP versus all other baselines to show a clear logical validity and visual grounding of the answers. The below example is the comparison between μ CRASP and the baselines at 50% **pruning**. Each row corresponds to a different example. Here we have excluded some of the baseline in the cases where they completely collapsed and outputs gibberish text. For instance in all of the below examples we have excluded result of magnitude pruning [22] for the aforementioned reasons.


<p>Question: What U.S. city is the most likely setting for this street?</p>	<p>FLAP: The generated response focuses on unrelated visual details such as lights, walls, and sky colour, failing to infer the city shown in the image. ...[truncated]</p>
	<p>LLM Pruner: The image is interpreted as an urban environment with buildings, entrances, and architectural structures. However, the generated reasoning fails to identify the explicit textual cue indicating New York City.</p>
<p>Ground Truth COT Trace: Step-by-Step Thought: 1. I observe the text “New York City Bus” displayed on the rear of the bus, indicating that the bus operates in New York City. 2. The architecture of the surrounding buildings and the design of the bus are also consistent with a typical New York City street environment. 3. Therefore, the most likely setting for this street is New York City. Final Answer: New York.</p>	<p>Wanda-SP: The generated response becomes repetitive and drifts into unrelated descriptions of roads, pavements, and people standing in the street scene. ...[truncated]</p>
<p>μCRASP (Ours): The image contains a bus with signage indicating “New York City Bus,” which strongly suggests that the scene takes place in New York City. The surrounding urban architecture and overall street layout are also visually consistent with a dense metropolitan setting such as New York. Final Answer: New York City.</p>	<p>Attribution Score Pruning: No output token generated.</p>

Figure 11: Qualitative comparison of reasoning traces under structured pruning on urban scene understanding tasks.

NeurIPS Paper Checklist

1. Claims

Question: Do the main claims made in the abstract and introduction accurately reflect the paper’s contributions and scope?

Answer: [Yes]

Justification: The main claims in the abstract and introduction have clearly reflected in the experimental results of the paper.

Guidelines:

- The answer [N/A] means that the abstract and introduction do not include the claims made in the paper.
- The abstract and/or introduction should clearly state the claims made, including the contributions made in the paper and important assumptions and limitations. A [No] or [N/A] answer to this question will not be perceived well by the reviewers.
- The claims made should match theoretical and experimental results, and reflect how much the results can be expected to generalize to other settings.


<p>Question: What colour is the frisbee?</p>	<p>FLAP: The light brown object being held suggests the person's clothing, which appears to be red.</p>
	<p>LLM Pruner: The image shows a blue background with a yellow circle on it.</p>
<p>Ground Truth COT Trace: Step-by-Step Thought: 1. I observe a bright yellow-green object in the air above the person, which appears to be a frisbee. 2. The frisbee's colour is distinctly greenish-yellow, matching the typical appearance of a frisbee. 3. Therefore, the colour of the Frisbee is green. Final Answer: green.</p>	<p>Wanda-SP: The image depicts a beach scene with rocks piled up to the right side of the beach. The ocean itself is visible in the middle ground. The shoreline is represented by the waves crashing on the sand. The shoreline is depicted as a curved line along the topmost part of the picture. The ocean itself is shown in the middle ground. The shoreline is represented by the curved line. The shoreline itself is depicted as a line. The shoreline itself is shown as a line. The ocean itself is shown as a line. The shoreline itself is shown as a line. The shoreline itself is shown.</p>
<p>μCRASP (Ours): The frisbee in the image appears to be yellow with some green markings, which is typical of a standard frisbee used in beach settings or similar environments. Final colour: Yellow with green markings.</p>	<p>Attribution Score Pruning: andy Rencontre blue Rencontre pione Rencontre espos</p>

Figure 12: Qualitative comparison of reasoning traces under structured pruning.

- It is fine to include aspirational goals as motivation as long as it is clear that these goals are not attained by the paper.

2. Limitations

Question: Does the paper discuss the limitations of the work performed by the authors?

Answer: [Yes]

Justification: We have added the limitations in the paper, including some lightweight heuristic that we followed in the work to craft our algorithm. We have also included additional technical limitations at the end of the main paper.

Guidelines:

- The answer [N/A] means that the paper has no limitation while the answer [No] means that the paper has limitations, but those are not discussed in the paper.
- The authors are encouraged to create a separate “Limitations” section in their paper.
- The paper should point out any strong assumptions and how robust the results are to violations of these assumptions (e.g., independence assumptions, noiseless settings, model well-specification, asymptotic approximations only holding locally). The authors should reflect on how these assumptions might be violated in practice and what the implications would be.


<p>Question: How many people are in the picture?</p>	<p>FLAP: In this image, the model output becomes fragmented and incoherent. Based on the visible text, the response appears truncated and fails to produce a valid counting answer. ...[truncated]</p>
	<p>LLM Pruner: The image shows a snowy landscape with multiple figures, some of whom appear to depict an outdoor winter scene. The central figure is wearing a red outfit, indicating a skiing activity. Therefore, the answer is that there are no people depicted as individuals being counted correctly.</p>
<p>Ground Truth COT Trace: Step-by-Step Thought: 1. I observe four individuals seated in a ski lift chair. 2. Each person is wearing winter clothing and appears to be enjoying the ride. 3. Therefore, the total number of people in the picture is four. Final Answer: four.</p>	<p>Wanda-SP: The generated response becomes highly corrupted and contains fragmented tokens without meaningful semantic structure. ...[truncated]</p>
<p>μCRASP (Ours): There are four people in the picture. The image shows a group of individuals sitting together on a ski lift, which is a common mode of transport used to carry skiers or snow riders. Each person appears to be wearing winter or snow gear, and they are all facing towards the camera, indicating that they are likely part of the same group. Final answer from the image and question: four.</p>	<p>Attribution Score Pruning: Rencontre onaut Rencontre Rencontre pione Rencontre beitendia ros espos. ...[truncated]</p>

Figure 13: Qualitative comparison of reasoning traces under structured pruning on counting-based multimodal reasoning examples.

- The authors should reflect on the scope of the claims made, e.g., if the approach was only tested on a few datasets or with a few runs. In general, empirical results often depend on implicit assumptions, which should be articulated.
- The authors should reflect on the factors that influence the performance of the approach. For example, a facial recognition algorithm may perform poorly when image resolution is low or images are taken in low lighting. Or a speech-to-text system might not be used reliably to provide closed captions for online lectures because it fails to handle technical jargon.
- The authors should discuss the computational efficiency of the proposed algorithms and how they scale with dataset size.
- If applicable, the authors should discuss possible limitations of their approach to address problems of privacy and fairness.
- While the authors might fear that complete honesty about limitations might be used by reviewers as grounds for rejection, a worse outcome might be that reviewers discover limitations that aren't acknowledged in the paper. The authors should use their best judgment and recognize that individual actions in favor of transparency play an important role in developing norms that preserve the integrity of the community. Reviewers will be specifically instructed to not penalize honesty concerning limitations.

3. Theory assumptions and proofs



Figure 14: Qualitative comparison of reasoning traces under structured pruning on object counting tasks.

Question: For each theoretical result, does the paper provide the full set of assumptions and a complete (and correct) proof?

Answer: [No]

Justification: [N/A]

Guidelines: This paper proposes an empirical structured pruning framework and does not present any formal theoretical results, theorems, lemmas, or proofs. All claims are supported by experimental evidence across four VLMs and three reasoning benchmarks.

- The answer [N/A] means that the paper does not include theoretical results.
- All the theorems, formulas, and proofs in the paper should be numbered and cross-referenced.
- All assumptions should be clearly stated or referenced in the statement of any theorems.

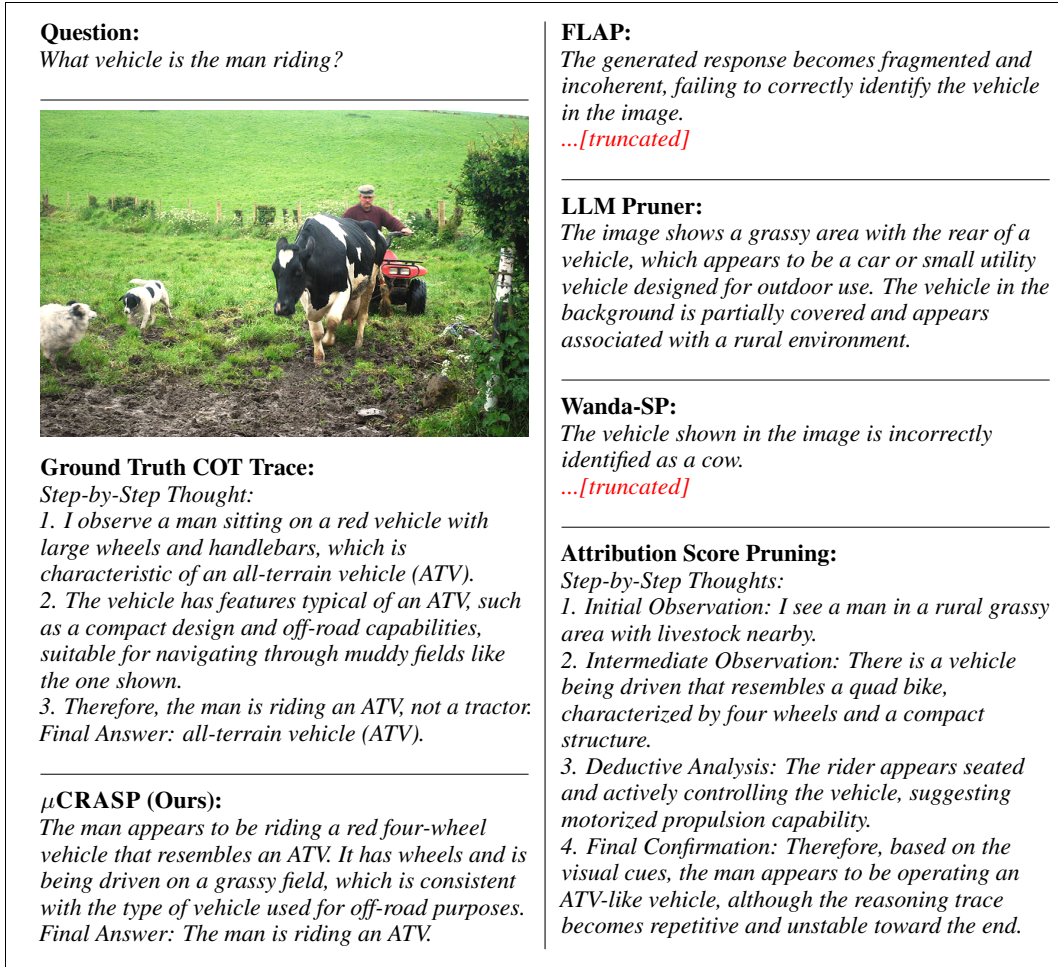


Figure 15: Qualitative comparison of reasoning traces under structured pruning on vehicle identification tasks.

- The proofs can either appear in the main paper or the supplemental material, but if they appear in the supplemental material, the authors are encouraged to provide a short proof sketch to provide intuition.
- Inversely, any informal proof provided in the core of the paper should be complemented by formal proofs provided in appendix or supplemental material.
- Theorems and Lemmas that the proof relies upon should be properly referenced.

4. Experimental result reproducibility

Question: Does the paper fully disclose all the information needed to reproduce the main experimental results of the paper to the extent that it affects the main claims and/or conclusions of the paper (regardless of whether the code and data are provided or not)?

Answer: [Yes]

Justification: The implementation details of our main experimental results with all hyper-parameters and the hardware resources are included in the appendix.

Guidelines:

- The answer [N/A] means that the paper does not include experiments.
- If the paper includes experiments, a [No] answer to this question will not be perceived well by the reviewers: Making the paper reproducible is important, regardless of whether the code and data are provided or not.

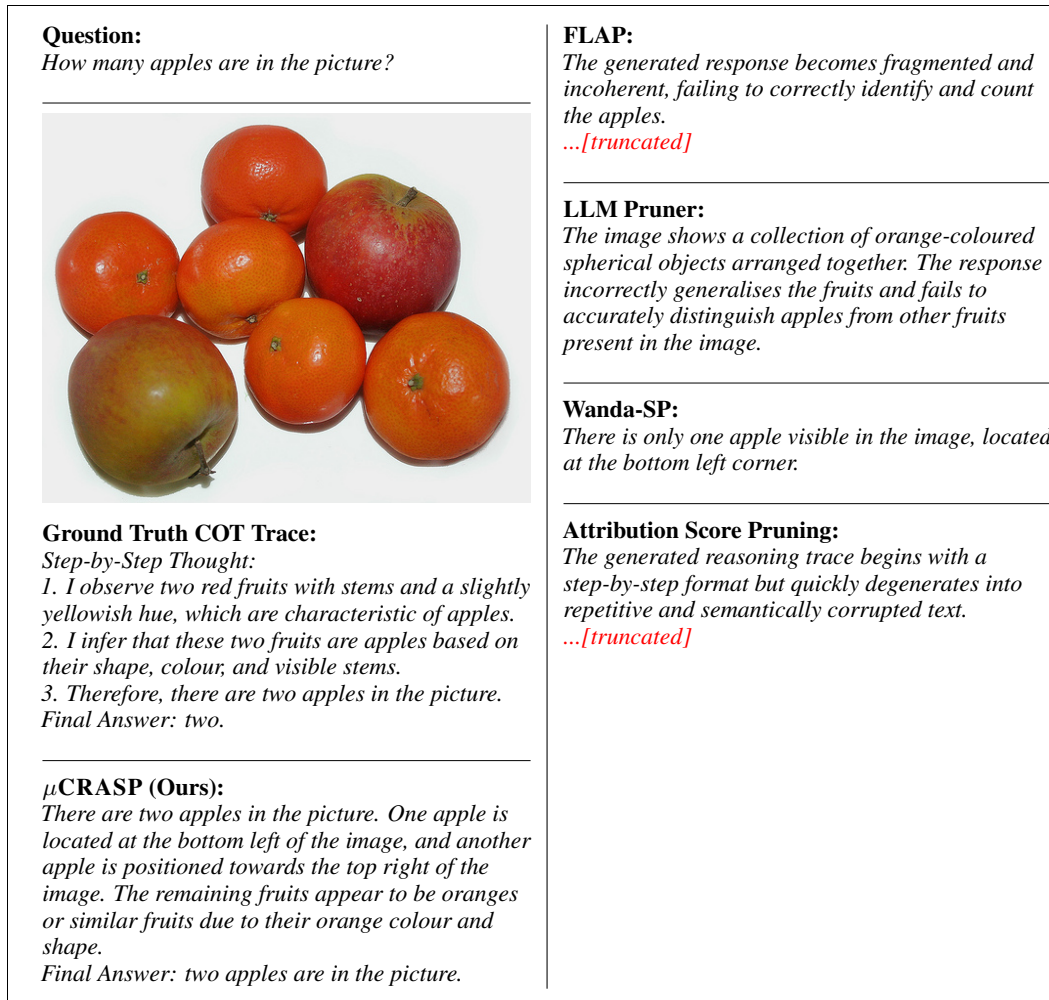


Figure 16: Qualitative comparison of reasoning traces under structured pruning on fruit counting tasks.

- If the contribution is a dataset and/or model, the authors should describe the steps taken to make their results reproducible or verifiable.
- Depending on the contribution, reproducibility can be accomplished in various ways. For example, if the contribution is a novel architecture, describing the architecture fully might suffice, or if the contribution is a specific model and empirical evaluation, it may be necessary to either make it possible for others to replicate the model with the same dataset, or provide access to the model. In general, releasing code and data is often one good way to accomplish this, but reproducibility can also be provided via detailed instructions for how to replicate the results, access to a hosted model (e.g., in the case of a large language model), releasing of a model checkpoint, or other means that are appropriate to the research performed.
- While NeurIPS does not require releasing code, the conference does require all submissions to provide some reasonable avenue for reproducibility, which may depend on the nature of the contribution. For example
 - (a) If the contribution is primarily a new algorithm, the paper should make it clear how to reproduce that algorithm.
 - (b) If the contribution is primarily a new model architecture, the paper should describe the architecture clearly and fully.


<p>Question: What colour is the man's shirt?</p>	<p>FLAP: The response incorrectly describes a person in red standing against an orange background, failing to identify the actual shirt colour in the image.</p>
	<p>LLM Pruner: The image depicts a grassy outdoor setting with fenced areas and cows grazing nearby. The generated response focuses primarily on the environment and fails to answer the shirt-colour question.</p>
<p>Ground Truth COT Trace: Step-by-Step Thought: 1. I observe a man standing between two fenced areas containing cows. 2. The man is wearing a light-coloured shirt, which appears to be yellow. 3. Therefore, the colour of the man's shirt is yellow. Final Answer: yellow.</p>	<p>Wanda-SP: The man in the image is described as wearing a blue shirt, which is incorrect.</p>
<p>μCRASP (Ours): The man in the image is wearing a light-coloured shirt, which appears to be yellow or a similar shade. This can be inferred from the visible details of his clothing in the image. Final colour: yellow.</p>	<p>Attribution Score Pruning: black farm animal green Rencontre espous be ...[truncated]</p>

Figure 17: Qualitative comparison of reasoning traces under structured pruning on colour identification tasks.

- (c) If the contribution is a new model (e.g., a large language model), then there should either be a way to access this model for reproducing the results or a way to reproduce the model (e.g., with an open-source dataset or instructions for how to construct the dataset).
- (d) We recognize that reproducibility may be tricky in some cases, in which case authors are welcome to describe the particular way they provide for reproducibility. In the case of closed-source models, it may be that access to the model is limited in some way (e.g., to registered users), but it should be possible for other researchers to have some path to reproducing or verifying the results.

5. Open access to data and code

Question: Does the paper provide open access to the data and code, with sufficient instructions to faithfully reproduce the main experimental results, as described in supplemental material?

Answer: [No]

Justification: Since we have conducted extensive experiments on several datasets, providing detailed scripts is intricate. The code will be made available upon acceptance of the work.

Guidelines:

Guidelines:

- The answer [N/A] means that paper does not include experiments requiring code.
- Please see the NeurIPS code and data submission guidelines (<https://neurips.cc/public/guides/CodeSubmissionPolicy>) for more details.

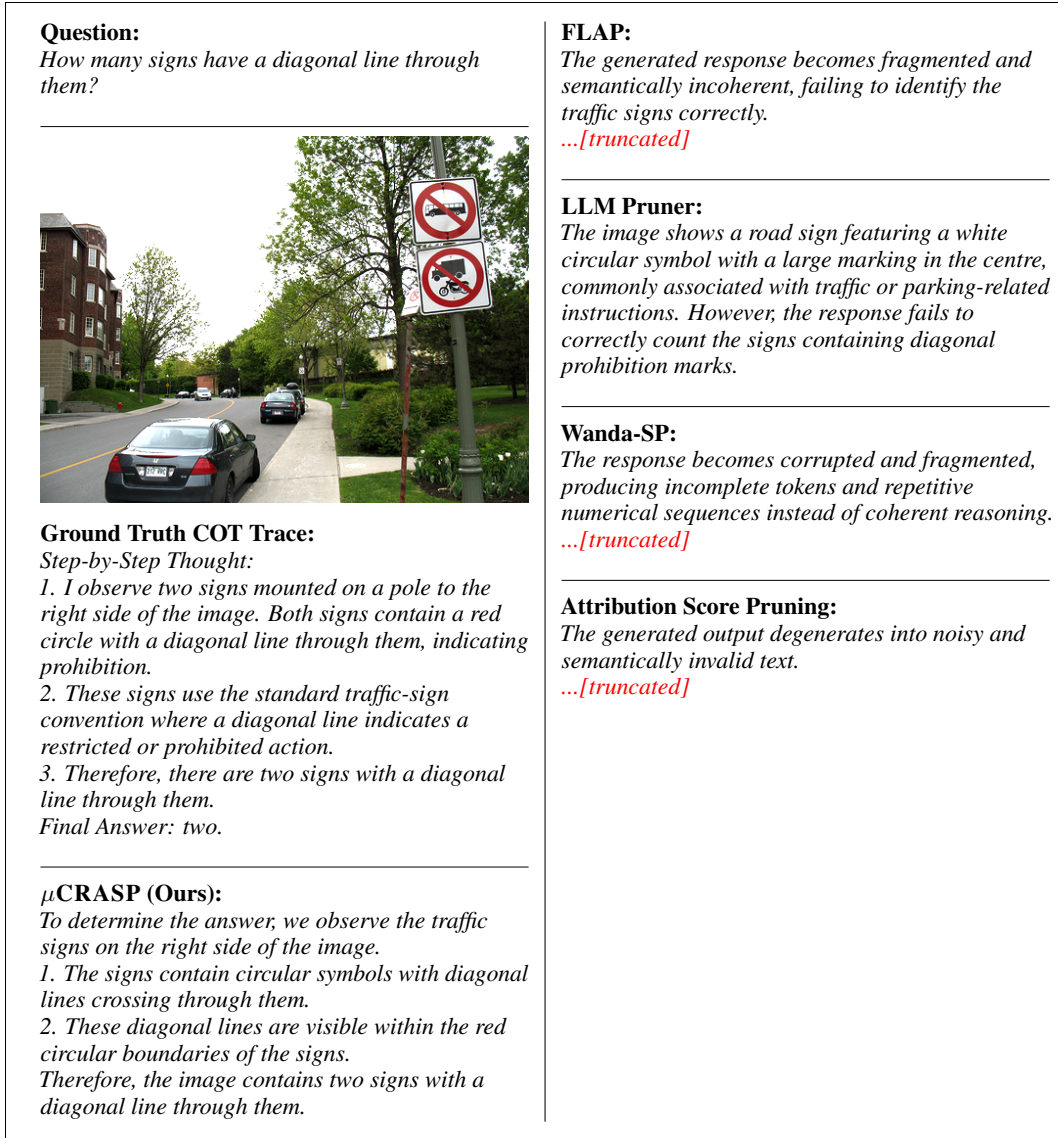


Figure 18: Qualitative comparison of reasoning traces under structured pruning on traffic-sign reasoning tasks.

- While we encourage the release of code and data, we understand that this might not be possible, so [No] is an acceptable answer. Papers cannot be rejected simply for not including code, unless this is central to the contribution (e.g., for a new open-source benchmark).
- The instructions should contain the exact command and environment needed to run to reproduce the results. See the NeurIPS code and data submission guidelines (<https://neurips.cc/public/guides/CodeSubmissionPolicy>) for more details.
- The authors should provide instructions on data access and preparation, including how to access the raw data, preprocessed data, intermediate data, and generated data, etc.
- The authors should provide scripts to reproduce all experimental results for the new proposed method and baselines. If only a subset of experiments are reproducible, they should state which ones are omitted from the script and why.
- At submission time, to preserve anonymity, the authors should release anonymized versions (if applicable).


<p>Question: What is likely the mascot of the team whose website address appears in the background?</p>	<p>FLAP: The generated response becomes fragmented and semantically incoherent, failing to correctly infer the mascot from the website text in the background. ...[truncated]</p>
	<p>LLM Pruner: The image shows a baseball field with a player in uniform, suggesting a sports-related environment. However, the generated response focuses only on the baseball setting and fails to infer the mascot associated with the website text displayed in the background.</p>
<p>Ground Truth COT Trace: Step-by-Step Thought: 1. I observe the text “workbears.com” displayed prominently on the outfield wall in the background. 2. The term “bears” in the website address suggests that the team’s mascot is likely a bear, since sports team mascots commonly reflect the team name or theme. 3. Therefore, the mascot of the team is likely a bear. Final Answer: bear.</p>	<p>Wanda-SP: The generated reasoning trace becomes repetitive and unstable, drifting into unrelated descriptions of photography equipment, clubhouses, and baseball terminology. ...[truncated]</p>
<p>μCRASP (Ours): To determine the likely mascot of the team, I observe that the background contains a prominent advertisement displaying the text “workbears.com”. The presence of the word “bears” strongly suggests that the associated team mascot is a bear. Final Answer: bear.</p>	<p>Attribution Score Pruning: Step 1: Observation: The website address displayed on the stadium signage suggests a possible team affiliation or sponsorship. Step 2: Intermediate Reasoning: The generated response attempts to connect the signage with the identity of the team but becomes repetitive and semantically unstable. Step 3: Final Reasoning: The reasoning trace degenerates into repeated connector phrases without reaching a coherent final answer. ...[truncated]</p>

Figure 19: Qualitative comparison of reasoning traces under structured pruning on contextual mascot inference tasks.

- Providing as much information as possible in supplemental material (appended to the paper) is recommended, but including URLs to data and code is permitted.

6. Experimental setting/details

Question: Does the paper specify all the training and test details (e.g., data splits, hyperparameters, how they were chosen, type of optimizer) necessary to understand the results?

Answer: [Yes]

Justification: All the datasets used and their split sizes, as well as the detailed experimental setup we have included in the appendix. that has been open-sourced.

Guidelines:

- The answer [N/A] means that the paper does not include experiments.
- The experimental setting should be presented in the core of the paper to a level of detail that is necessary to appreciate the results and make sense of them.
- The full details can be provided either with the code, in appendix, or as supplemental material.

7. Experiment statistical significance

Question: Does the paper report error bars suitably and correctly defined or other appropriate information about the statistical significance of the experiments?

Answer: [Yes]

Justification: We have discussed it in the appendix.

Guidelines:

- The answer [N/A] means that the paper does not include experiments.
- The authors should answer [Yes] if the results are accompanied by error bars, confidence intervals, or statistical significance tests, at least for the experiments that support the main claims of the paper.
- The factors of variability that the error bars are capturing should be clearly stated (for example, train/test split, initialization, random drawing of some parameter, or overall run with given experimental conditions).
- The method for calculating the error bars should be explained (closed form formula, call to a library function, bootstrap, etc.)
- The assumptions made should be given (e.g., Normally distributed errors).
- It should be clear whether the error bar is the standard deviation or the standard error of the mean.
- It is OK to report 1-sigma error bars, but one should state it. The authors should preferably report a 2-sigma error bar than state that they have a 96% CI, if the hypothesis of Normality of errors is not verified.
- For asymmetric distributions, the authors should be careful not to show in tables or figures symmetric error bars that would yield results that are out of range (e.g., negative error rates).
- If error bars are reported in tables or plots, the authors should explain in the text how they were calculated and reference the corresponding figures or tables in the text.

8. Experiments compute resources

Question: For each experiment, does the paper provide sufficient information on the computer resources (type of compute workers, memory, time of execution) needed to reproduce the experiments?

Answer: [Yes]

Justification: We have mentioned the detailed breakdown of the hardware we used along with their compute time for this work.

Guidelines:

- The answer [N/A] means that the paper does not include experiments.
- The paper should indicate the type of compute workers CPU or GPU, internal cluster, or cloud provider, including relevant memory and storage.
- The paper should provide the amount of compute required for each of the individual experimental runs as well as estimate the total compute.
- The paper should disclose whether the full research project required more compute than the experiments reported in the paper (e.g., preliminary or failed experiments that didn't make it into the paper).

9. Code of ethics

Question: Does the research conducted in the paper conform, in every respect, with the NeurIPS Code of Ethics <https://neurips.cc/public/EthicsGuidelines>?

Answer: [Yes]

Justification: We have carefully checked and followed the NeurIPS Code of Ethics.

Guidelines:

- The answer [N/A] means that the authors have not reviewed the NeurIPS Code of Ethics.
- If the authors answer [No], they should explain the special circumstances that require a deviation from the Code of Ethics.

- The authors should make sure to preserve anonymity (e.g., if there is a special consideration due to laws or regulations in their jurisdiction).

10. Broader impacts

Question: Does the paper discuss both potential positive societal impacts and negative societal impacts of the work performed?

Answer: [Yes]

Justification: Our work develops a structured pruning framework that compresses vision-language models while preserving chain-of-thought reasoning quality. The primary positive societal impact is enabling deployment of capable multi-modal reasoning models on resource-constrained hardware. We have discussed this in the appendix.

Guidelines:

- The answer [N/A] means that there is no societal impact of the work performed.
- If the authors answer [N/A] or [No], they should explain why their work has no societal impact or why the paper does not address societal impact.
- Examples of negative societal impacts include potential malicious or unintended uses (e.g., disinformation, generating fake profiles, surveillance), fairness considerations (e.g., deployment of technologies that could make decisions that unfairly impact specific groups), privacy considerations, and security considerations.
- The conference expects that many papers will be foundational research and not tied to particular applications, let alone deployments. However, if there is a direct path to any negative applications, the authors should point it out. For example, it is legitimate to point out that an improvement in the quality of generative models could be used to generate Deepfakes for disinformation. On the other hand, it is not needed to point out that a generic algorithm for optimizing neural networks could enable people to train models that generate Deepfakes faster.
- The authors should consider possible harms that could arise when the technology is being used as intended and functioning correctly, harms that could arise when the technology is being used as intended but gives incorrect results, and harms following from (intentional or unintentional) misuse of the technology.
- If there are negative societal impacts, the authors could also discuss possible mitigation strategies (e.g., gated release of models, providing defenses in addition to attacks, mechanisms for monitoring misuse, mechanisms to monitor how a system learns from feedback over time, improving the efficiency and accessibility of ML).

11. Safeguards

Question: Does the paper describe safeguards that have been put in place for responsible release of data or models that have a high risk for misuse (e.g., pre-trained language models, image generators, or scraped datasets)?

Answer: [N/A]

Justification: The paper poses no such risks.

Guidelines:

- The answer [N/A] means that the paper poses no such risks.
- Released models that have a high risk for misuse or dual-use should be released with necessary safeguards to allow for controlled use of the model, for example by requiring that users adhere to usage guidelines or restrictions to access the model or implementing safety filters.
- Datasets that have been scraped from the Internet could pose safety risks. The authors should describe how they avoided releasing unsafe images.
- We recognize that providing effective safeguards is challenging, and many papers do not require this, but we encourage authors to take this into account and make a best faith effort.

12. Licenses for existing assets

Question: Are the creators or original owners of assets (e.g., code, data, models), used in the paper, properly credited and are the license and terms of use explicitly mentioned and properly respected?

Answer: [Yes]

Justification: We attribute the original owners of the data and code.

Guidelines:

- The answer [N/A] means that the paper does not use existing assets.
- The authors should cite the original paper that produced the code package or dataset.
- The authors should state which version of the asset is used and, if possible, include a URL.
- The name of the license (e.g., CC-BY 4.0) should be included for each asset.
- For scraped data from a particular source (e.g., website), the copyright and terms of service of that source should be provided.
- If assets are released, the license, copyright information, and terms of use in the package should be provided. For popular datasets, paperswithcode.com/datasets has curated licenses for some datasets. Their licensing guide can help determine the license of a dataset.
- For existing datasets that are re-packaged, both the original license and the license of the derived asset (if it has changed) should be provided.
- If this information is not available online, the authors are encouraged to reach out to the asset's creators.

13. **New assets**

Question: Are new assets introduced in the paper well documented and is the documentation provided alongside the assets?

Answer: [N/A]

Justification: No new assets were introduced in this work.

Guidelines:

- The answer [N/A] means that the paper does not release new assets.
- Researchers should communicate the details of the dataset/code/model as part of their submissions via structured templates. This includes details about training, license, limitations, etc.
- The paper should discuss whether and how consent was obtained from people whose asset is used.
- At submission time, remember to anonymize your assets (if applicable). You can either create an anonymized URL or include an anonymized zip file.

14. **Crowdsourcing and research with human subjects**

Question: For crowdsourcing experiments and research with human subjects, does the paper include the full text of instructions given to participants and screenshots, if applicable, as well as details about compensation (if any)?

Answer: [N/A]

Justification: The paper does not involve crowdsourcing experiments.

Guidelines:

- The answer [N/A] means that the paper does not involve crowdsourcing nor research with human subjects.
- Including this information in the supplemental material is fine, but if the main contribution of the paper involves human subjects, then as much detail as possible should be included in the main paper.
- According to the NeurIPS Code of Ethics, workers involved in data collection, curation, or other labor should be paid at least the minimum wage in the country of the data collector.

15. **Institutional review board (IRB) approvals or equivalent for research with human subjects**

Question: Does the paper describe potential risks incurred by study participants, whether such risks were disclosed to the subjects, and whether Institutional Review Board (IRB) approvals (or an equivalent approval/review based on the requirements of your country or institution) were obtained?

Answer: [N/A]

Justification: The paper does not involve crowdsourcing nor research with human subjects.

Guidelines:

- The answer [N/A] means that the paper does not involve crowdsourcing nor research with human subjects.
- Depending on the country in which research is conducted, IRB approval (or equivalent) may be required for any human subjects research. If you obtained IRB approval, you should clearly state this in the paper.
- We recognize that the procedures for this may vary significantly between institutions and locations, and we expect authors to adhere to the NeurIPS Code of Ethics and the guidelines for their institution.
- For initial submissions, do not include any information that would break anonymity (if applicable), such as the institution conducting the review.

16. Declaration of LLM usage

Question: Does the paper describe the usage of LLMs if it is an important, original, or non-standard component of the core methods in this research? Note that if the LLM is used only for writing, editing, or formatting purposes and does *not* impact the core methodology, scientific rigor, or originality of the research, declaration is not required.

Answer: [Yes].

Justification: We have used GPT-3.5 and GPT 4o for generation and LLM-as-judge metric.

Guidelines: We have properly mentioned use of LLMs in the metrics section of the paper. We have used LLM-Judge as one of our key metrics to evaluate the model generated Chain-of-Thought (CoT).

- The answer [N/A] means that the core method development in this research does not involve LLMs as any important, original, or non-standard components.
- Please refer to our LLM policy in the NeurIPS handbook for what should or should not be described.